AAiT
ADDIS ABABA INSTITUTE OF TECHNOLOGY
አዲስ አበባ ቴክኖሎጂ ኢንስቲትዩት
ADDIS ABABA UNIVERSITY
አዲስ አበባ ዩኒቨርሲቲ

ARCE

Addis Ababa University
Addis Ababa Institute of Technology
African Railway Center of Excellence

Behavior of Addis Ababa Light Rail Transit Embankments under Seasonal Changes in Suction

Tewodros Gemechu Bile

A Thesis Submitted in Partial Fulfillment of the Requirements for the Degree of Master of Science in Railway Engineering (Civil Infrastructure)

June 2023
Addis Ababa, Ethiopia

Dedication

To my wife Mahder Aman and my son Aaron Tewodros without whom this thesis would have been completed much, much, much earlier ☺

The undersigned have examined the thesis entitled '**Behavior of Addis Ababa Light Rail Transit Embankments under Seasonal Changes in Suction**' presented by **Tewodros Gemechu Bile**, a candidate for the degree of **Master of Science** and hereby certify that it is worthy of acceptance.

Dr. Tezera Firew Azmatch		
Advisor	Signature	Date
Dr. Tensay GebreMedhin		
Internal Examiner	Signature	Date
Dr. Henok Fikre		
External Examiner	Signature	Date
Mr. Kejela Temesgen		
Chairperson	Signature	Date

Undertaking

I certify that this research work titled “Behavior of Addis Ababa Light Rail Transit Embankments under Seasonal Changes in Suction” is my own work. The work has not been presented elsewhere for assessment. Where material has been used from other sources, it has been properly acknowledged / referred to.

Tewodros Gemechu Bile

Abstract

This research paper presents research on the behavior of selected embankment sections along the Addis Ababa Light Rail Transit (LRT) experiencing matric suction variation due to seasonal changes. In this study, an extended Mohr-Coulomb soil model in the MIDAS GTX NS software has been utilized to analyze the effect of precipitation on matric suction and by extension on slope stability and settlement prediction of a railway embankment along the North-South direction of the AALRT. The software implementation of the model was initially verified using an already published research on slope stability analysis of unsaturated soil. Climate data analysis has been conducted for a 40-year rainfall data acquired from the Ethiopian Meteorological Agency. Spatial and temporal simulation of matric suction variation has been carried out. The investigation's findings demonstrated that utilizing rainfall observations in the finite element analysis, it is possible to accurately anticipate how the matric suction distribution profile changes over time in an embankment. Results further indicate that as matric suction diminishes, stability is compromised, and settlement increases due to the upsurge in intensity, duration, and frequency of rainfall. The analysis's findings also indicate that one of the most crucial variables influencing rainfall infiltration for unsaturated slopes is rainfall intensity. It has also been made apparent that matric suction (and by extension slope stability and settlement) is highly affected by the location of ground water table. The factor of safety is amplified with raising depth of ground water table. Therefore, establishing the actual GWT is crucial in analysis and monitoring of actual embankments.

Key words: Embankment, Matric Suction, Settlement, Stability, Subgrade, Suction, SWCC

Acknowledgement

I am extremely grateful to the African Railway Center of Excellence (ARCE) for providing me a scholarship to study at the Center.

I am forever indebted to my advisor Dr. Tezera Firew Azmatch for his valuable insights and dedicated mentorship throughout this thesis work. This endeavor would not have been possible without his sensible and seasoned guidance. He has been nothing short of an ideal teacher, mentor, and thesis supervisor, offering advice and encouragement with the perfect blend of insight and humor.

Dr. Belete Birhanu has helped me a lot to carry out the climate analysis and I am very grateful for that. From Engineering Hydrology instructor to becoming a mentor, he has greatly affected my life in a very positive way. I salute him for his pure academic, professional, and personal excellence. What a delightful human being he is!

I am also grateful to my colleague Leamlak Minwuyelet for his overall technical support in addition to graciously lending me his high-performance computer along with genuine MIDAS software for analysis works. A very warm thanks is also in order for my other colleague Anteneh Mitiku who kindly helped out a lot with the laboratory works.

Special thanks must go out to my family who impacted and inspired me in ways I could not have envisaged and who stood by me through thick & thin enduring this long process with me, always offering support and love.

Galatoma!

አመሰግናለሁ!

Thank you!

Contents

Acronyms

AAiT – Addis Ababa Institute of Technology

AARC – Addis Ababa Red Clay

AAU – Addis Ababa University

AREMA – American Railway Engineering and Maintenance-of-Way Association

BBM - Barcelona Basic Model

CSL – Critical State Line

EMCM – Extended Mohr-Coulomb Model

FEM – Finite Element Method

GCM – Glasgow Coupled Model

GSD – Grain Size Distribution

IDF – Intensity Duration Frequency

LC – Loading Collapse Curve

LEM – Limit Equilibrium Method

LRT – Light Rail Transit

MCCM – Modified Cam Clay Model

MDD – Maximum Dry Density

MSSA – Modified State-Surface Approach

NCL – Normal Compression Loading

NGL – Natural Ground Level

OMC – Optimum Moisture Content

PI – Plasticity Index

List of Tables

List of Figures

1. Introduction

1.1 Background

Civil engineers, particularly geotechnical engineers, have traditionally been interested in the interactions between the atmosphere and the Earth. Certain interactions can be quick and devastating, leading to the destruction of structures like dams and bridges, as well as loss of life and severe environmental disasters. Other interactions can be slow and insidious, but they can still be harmful and costly in the long run. One of these interactions which could be characterized as devious is the interaction between the atmosphere and soil in the context of unsaturated soil mechanics as highlighted by (Blight, 1997).

It has been all but a perennial wisdom among practicing engineers to assume fully saturated soil conditions as the most conservative approach to analysing and designing a broad variety of geosystems (Briaud, J.L., 2013). Recent studies related to the stability of an initially unsaturated trench and a compacted unsaturated embankment show that failures are likely to occur due to the loss of matric suction with infiltration conditions prior to saturated condition.

Climate-sensitive geotechnical structures, such as earth dams, fills, and road and railway embankments, see seasonal fluctuations in water content (or suction) due to infiltration and evaporation. Railway embankments are usually exposed to the atmosphere, and their layers are generally in unsaturated conditions. The embankment materials in tropical regions such as Ethiopia are subjected to seasonal changes and large variations in water content. The water content change renders the material to be characterized as unsaturated and subjects it to different levels of matric suction.

Several researches [(A. S. O'Brien, 2004), (Cho & Lee, 2001) (J.M. Scott) (Ng & Shi, 1998) (Ni An, 2017) (Oh, Vanapalli, Qi, & Han, 2016) (Pradel & Raad, 1993) (R Cardaso, 2015) (Rafaela Cardoso, 2007) (S. Glendinning P. H., 2014) (Y.J. Cui, 2010) (Zhigang Cao, 2020)] have been done elsewhere on the topic but never in the context of Ethiopia. Numerous studies have looked at numerical simulations of rainwater infiltration and the subsequent slope instability.

Understanding infiltration rates and their contributions to water content, pore-water pressure fluctuations in the slope governed by the physical characteristics of the soil, and climatic factors are all necessary for the application of seepage and slope stability calculations. The mechanism and impact of precipitation infiltration into an unsaturated soil slope may be understood, and a viable method for slope stability analysis under transitory seepage from rainfall can be created. Geotechnical engineers are interested in this process because it can help them identify preventative solutions for slope failures brought on by rainfall. Rainfall plays the most important role in triggering of slope failure because infiltration of rainwater into a slope increases the moisture content and weight of subsoil and reduces the effective stress, thus making the slope unstable. Practice employs the total precipitation data since the beginning of one rainfall event (in other words, rainfall intensity and its duration time) as well as current rainfall intensity. Even though it is assumed that geotechnical structures are designed assuming the conditions of saturated soil state, in practice, the contribution of matric suction to slope and trench stability is heavily utilized. This is apparent since many of the excavations done in cohesive soils of Addis Ababa are conducted in a manner that ignores the provision of temporary support systems since the soil is “strong” enough to stand by itself as deep as 10 m.

The process of rainwater infiltration into an unsaturated railway embankment in Ethiopia and the impact of the infiltrated rainwater on changes in soil water content and pore-water pressure, which regulate the stability of a slope and the resulting settlement, do not appear to have been studied. The loss of matric suction brought on by rainfall infiltration is the cause of the instability of unsaturated soil slopes. Therefore, it is essential to estimate the fluctuation in matric suction caused by rainfall infiltration while analyzing the stability of unsaturated soil slopes. In this study, the fluctuation of matric suction related to rainwater infiltration for a railway embankment in an unsaturated soil was simulated using commercial finite element software, MIDAS GTX NS.

This paper is a culmination of the research works conducted at the junction of engineering hydrology, geotechnics and railway engineering. The study aims to investigate the influence of matric suction on the shear strength property and compression behavior of one local soil used as an embankment construction material in the Addis Ababa Light Rail Transit project.

1.2 Statement of the Problem

Slope failures due to rainfall are very frequent worldwide, and the damage caused by such failures is substantial. According to previous studies, rainfall can cause the development of a perched water table, a rise in the main groundwater level, surface erosion, and an increase in unit weight of soil due to a rise in moisture content [(Ng & Shi, 1998); (Cho & Lee, 2001)]. The assumption that slopes or trenches fail upon reaching only saturated conditions is not realistic. **Recent studies related to the stability of an initially unsaturated trench and a compacted unsaturated embankment show that failures are likely to occur due to the loss of matric suction with infiltration conditions prior to saturated condition.**

As a tropical country, Ethiopia experiences long, dry seasons followed by short but intense rainfall period. Although Ethiopia is among the least contributors of greenhouse gas emission, the country has been at the frontier of the notorious consequences of climate change. Rainfall is becoming increasingly erratic as heavy rainfall events appear to be more and more frequent, with changes in rainfall patterns, including decreased reliability and less predictability (Chemonic Inc. 2015). It goes without saying that this notorious attribute of climate change has serious implications on the safety and economy of railway embankment performance. This study presents the case for careful consideration of this phenomena in the design and construction of railway embankments by conducting stability analysis and settlement computation under extreme and erratic weather conditions.

1.3 Research Questions

- What are the updated values of intensity, duration, and frequency of rainfall in Addis Ababa city?
- How does the spatial and temporal evolution of the matric suction profile of the embankment look like?
- How does the stability of the embankment evolve under seasonal changes in suction?
- How much permanent settlement is predicted for the embankment under different conditions of matric suction?

1.4 Objectives of the Study

1.4.1 General Objective

This research generally aims to study the behavior (deformation and strength) of railway embankments under seasonal changes in suction on red clay embankment material along the Addis Ababa LRT.

1.4.2 Specific Objectives

- Generate an up-to-date IDF curve for Addis Ababa city
- Quantify the spatial and temporal variation of matric suction in the embankment soil.
- Stability analysis of the railway embankments under different IDF conditions therefore different suction levels.
- Settlement prediction of railway embankments under different IDF conditions therefore different suction levels.

1.5 Scope of the Study

The scope of this study is delineated at performance evaluation of the substructure for the project in question. Only one local subgrade material is carefully studied. The existence of a great variety of soils composing a railway track bed along its extension may be responsible for important differential vertical displacements along the longitudinal development of the rail. This paper presents a preliminary study where profiles with only one type of soil were investigated. The water retention curve of a soil evolves during compaction because the volume of pores decreases, pore sizes change, and the proportion of the void space in micro and macro pores changes. This dimension is out of the scope of this research. The study does not include field monitoring activities either. In this study the effect of matric suction cycle has been studied and its accumulation effect is entrusted for further research. Hysteresis and temporary ponding of precipitation are also outside of the scope of this thesis.

1.6 Limitations of the Study

The research assumes homogenous nature of soil in the study area. Moreover, the embankment and natural ground are assumed to be of the same red clay soil with the former assumed to being compacted to maximum dry density level. Infiltration analysis was performed on small unit volumes assumed to be homogeneous in soil characteristics. No dynamic analysis was performed in this study. Due to unavailability of unsaturated triaxial testing, empirical relationships have been utilized to circumvent the situation and come up with unsaturated properties of the soil in question. Power outages also interrupted several conventional triaxial tests. As such the researcher has opted to use secondary data to complement the primary experimental data.

1.7 Significance of the Study

Failures in railway embankment slopes have the potential to shut down sections of the transportation infrastructure, causing delays and, in the worst-case scenario, putting people's lives in danger. According to (S. Glendinning J. W., 2009), the cost of emergency repair is estimated to be 10 times that of planned maintenance. As a result, advancing our understanding of embankment aging and deterioration to the point where we can upgrade construction management and maintenance systems would have major financial and safety benefits for global infrastructure. The accumulation of seasonal displacements has a negative impact in track geometry and therefore its prediction can be useful for planning maintenance interventions. This study paves the way for such practice in a localized manner. The assessment will be used as an input for evaluating the effectiveness of the construction of Addis Ababa LRT.

The economic perspective for the need in adopting the practice of unsaturated soil mechanics makes a double fold appeal for tropical countries like Ethiopia. In many developing countries, infrastructure development makes up a key portion of the Growth Domestic Product (GDP). As such ensuring economy of design, construction and supervision works is/should be of high priority. This research helps to substantiate and amplify this call for sanity.

1.8 Organization of the Paper

This report is organized into five main chapters.

Chapter 1 Introduction – presents the background of the study, problem statement, research questions, objectives of the study, scope of the study, limitations of the study, significance of the study and organization of the research paper.

Chapter 2 Literature Review – encapsulates a review of relevant literature pertinent to the research in question. It is organized into theoretical literatures review and empirical literature review. A conceptual framework is presented at last as an amalgamation of the aforementioned review components in order to fill the research gap identified.

Chapter 3 Research Methodology – describes the research process undertaken to arrive at the sought after outputs. Data collection and/or generation techniques, analysis methods, result interpretation and presentation approaches have all been stated in this chapter.

Chapter 4 Results and Discussions – presents the processes of modelling the problem, analyzing it and results of the analysis, and further discussions and interpretation of the results,

Chapter 5 Conclusions and Recommendations – contains conclusions drawn from them and recommendations for future research.

2. Literature Review

2.1 Theoretical Literature Review

2.1.1 IDF Curves

The intensity-duration-frequency curves are used in hydrology to express in a synthetic way, fixed return period T and a duration d of a rainfall event, and for a given location, the information on the maximum rainfall height h and the maximum rainfall intensity i. Known these parameters, it is possible to build synthetic rain graphs that are useful to the elaboration of flood hydrographs. (Francesco De Paola, 2014)

An IDF is a three-parameter curve, in which intensity of a certain return period is related to duration of rainfall event. An IDF curve enables the hydrologists to develop hydrologic systems that consider worst-case scenarios of rainfall intensity and duration during a given interval of time. IDF analysis is used to capture the main characteristics of point rainfall for shorter durations. Such analysis provides an effective tool for statistically summarizing regional rainfall information, The IDF analysis starts by gathering time series records of different durations (in this study provided by weather generator). After time series data is gathered, annual extremes are extracted from the record for each duration. The annual extreme data is then fitted to a probability distribution, in order to estimate rainfall quantities.

2.1.2 Constitutive Modelling for Unsaturated Soils

A soil model is a mathematical representation of the behavior of the soil under load. The model typically relates the stresses applied to the strains experienced by the soil as a result. The simplest of these relationships is the theory of elasticity. (Jean-Louis Briaud, 2013) In the mechanics of materials, constitutive relations that are used to depict the mechanical behavior of materials are usually described in a stress space. Unlike concrete or steel, soil is a particulate material with little or no bonding between the particles. This complex particulate material, soil, must be modelled as if it were a continuum. (Wood, 1990) Because of this, the water pressures acting within the soil pores are just as important as the stresses

applied to its boundaries. This means that changes in the groundwater regime can be crucial in stabilizing, or destabilizing, a slope, retaining wall or foundation. (Schanz, 2007)
Soil mechanics principles are more established for soils in saturated states. As highlighted by several authors (Sheng, Fredlund, & Gens, 2008) (Antonio Gens, 2016), (Sheng D. , 2011), generalization of these principles to unsaturated soils requires careful consideration of the following fundamental issues: (1) volume change behavior associated with suction or saturation changes, (2) shear strength behavior associated with suction or saturation changes, and (3) hydraulic behavior associated with suction or saturation changes. Recent developments focus on the proposal of coupled hydraulic-mechanical models and the possibility of casting them in a sound thermodynamical framework. (Daichao Sheng, 2008)

Extended Mohr-Coulomb Model

Fredlund et al. (1978) formulated an extended M-C criterion to describe the shear strength behavior of unsaturated soil. The failure envelope is a planar surface in the space of the stress state variables $\sigma - u_a$ and $u_a - u_w$ and shear stress τ and may be written as

$$\tau_f = c' + (\sigma - u_a)_f \tan \phi' + (u_a - u_w)_f \tan \phi^b$$

where c' is the cohesion at zero matric suction and zero net normal stress, $(\sigma - u_a)_f$ is the net normal stress on the failure plane at failure, ϕ' is the angle of internal friction associated with the net normal stress variable, $(u_a - u_w)_f$ is the matric suction at failure, and ϕ^b is an internal friction angle associated with matric suction that describes the rate of increase in shear strength relative to matric suction.

The first two terms on the right-hand side of the equation describe the conventional M-C criterion for the strength of saturated soil. The third term captures the increase in shear strength with increasing matric suction in unsaturated soil. The corresponding failure surface for the extended M-C criterion is illustrated in the three-dimensional stress space in the figure below.

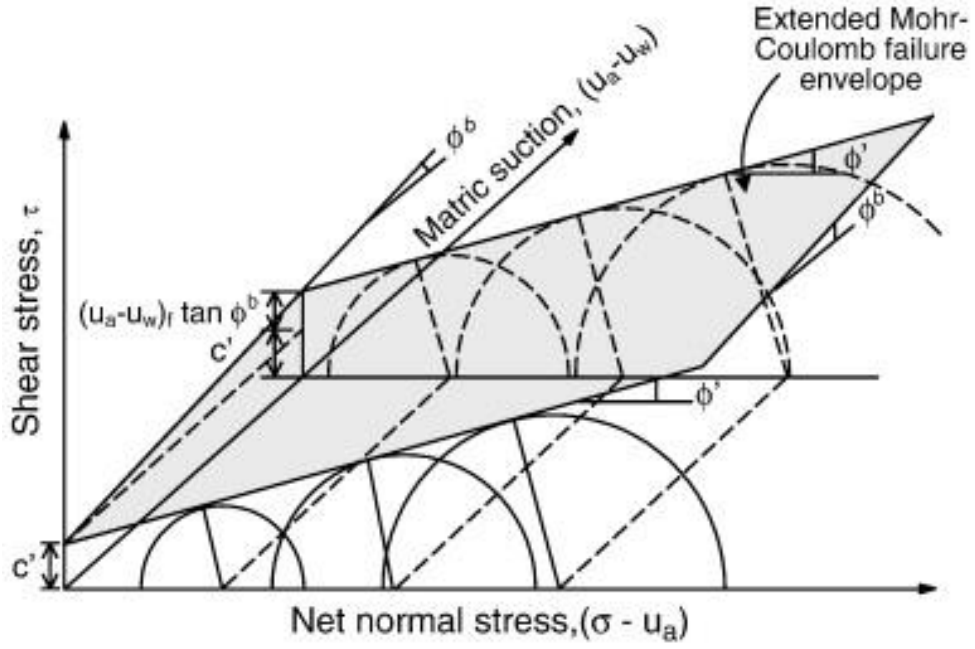

Figure 1 Extended Mohr-Coulomb failure envelope

Despite the simplicity of the extended M-C criterion for describing the strength of unsaturated soil, several important factors may limit its general validity over a wide range of matric suction. Most notably, there is significant experimental evidence showing that the angle describing the increase in shear strength with respect to matric suction ϕ^b is a highly nonlinear function of matric suction. The value of ϕ^b for a given soil can vary from a value equal or close to the internal friction angle ϕ' for suctions near zero (i.e., near the saturated condition) to as low as 0° or even negative values for suctions approaching the residual saturation state.

One logical way to describe the dependency of shear strength on matric suction is to follow the classical soil mechanics formalism using effective stress and the conventional M-C failure criterion. A practical advantage of the effective stress approach is that it remains firmly within the context of classical soil mechanics, thus requiring minimum modification to the existing elasto-plastic theories of stress-strain or constitutive laws that have been implemented in many numerical codes.

$$\sigma' = (\sigma - u_a) + \chi(u_a - u_w)$$

The effective stress parameter χ in Bishop's effective stress definition is a function of the degree of saturation of the soil mass and reflects the contribution of matric suction to

effective stress. For saturated soil, the air pressure is equal to zero, the water pressure is compressive or positive, $\mathcal{X}$ is equal to one, and the equation reduces to Terzaghi's classical effective stress equation: $\sigma' = (\sigma - u_w)$. For completely dry soil, $\mathcal{X}$ is equal to zero and the effective stress is the difference between total stress and air pressure: $\sigma' = (\sigma - u_a)$. For partially saturated soil, $\mathcal{X}$ is some function of the degree of saturation or matric suction.

The effective stress parameter $\mathcal{X}$ may not be directly measured or controlled through experiments. However, Bishop (1954) proposed an indirect way to obtain $\mathcal{X}$ from the stresses measured in soil specimens at failure. The traditional M-C criterion was used to represent the failure conditions: $\tau_f = c' + \sigma' \tan \phi'$ which after substitution of the effective stress expression leads to $\tau_f = c' + \left[(\sigma - u_a)_f + \mathcal{X}_f (u_a - u_w)_f\right] \tan \phi'$ where τ_f is shear strength and c' and ϕ' are the effective cohesion and friction angle, respectively.

Since the matric suction at failure may be used to indirectly define the degree of saturation by way of the soil-water characteristic curve, a one-to-one relationship between $\mathcal{X}$ and degree of saturation can be established. Following this general strategy, Bishop (1959) proposed a nonlinear form of $\mathcal{X}$ based on direct shear tests taken to failure, as a function of degree of saturation. In the extended M-C criterion, matric suction is used as an independent stress state variable along with net normal stress for describing unsaturated shear strength. On one hand, introducing the constant internal friction angle with respect to matric suction ϕ^b provides a relatively simple mathematical and graphical representation of the shear strength envelope. Reconciliation between Bishop's effective stress concept and the extended M-C criterion can be achieved by an alternative approach for describing the state of stress and strength in unsaturated soil. The M-C criterion incorporating both Bishop's effective stress and the suction stress concept expressed by the equation:

$$\tau_f = c' + \left[(\sigma - u_a)_f + \mathcal{X}_f (u_a - u_w)_f\right] \tan \phi'$$

can be rearranged as

$$\tau_f = c' + \mathcal{X}_f (u_a - u_w)_f \tan \phi' + (\sigma - u_a)_f \tan \phi' = c' + c'' + (\sigma - u_a)_f \tan \phi'$$

where $c'' = \mathcal{X}_f (u_a - u_w)_f \tan \phi'$

(Lu and Likos, 2004)

Barcelona Basic Model (BBM)

The BBM is an elastic plastic strain hardening model that makes use of two stress variables: the net normal stress ($p^* = \sigma - u_a$) and the net water tension or suction ($s = u_w - u_a$). The model is based on several observations of the behavior of unsaturated soils, including reversible swelling and shrinking at low confining pressures, collapse at high pressures, and increase in yield stress (preconsolidation pressure) with increase in net water tension. BBM becomes equal to the Modified Cam Clay model when the suction is equal to zero. Like the MCC model, the BBM uses a linear relationship between the void ratio e and the natural logarithm of the net normal stress p^*, called the normal compression loading (NCL) curve. The BBM adds another NCL curve with a linear relationship between the void ratio e and the natural logarithm of the net water tension or suction s.

The Barcelona Basic Model (BBM) proposed by Alonso et al. (1990) has had a pioneering role and is one of the few elasto-plastic constitutive models for unsaturated soils which have seen relatively widespread implementation into finite element codes and application to real boundary value problems (Alonso, 1990) (Daichao Sheng, 2008). However, there are no well-established methods for selecting parameter values in the BBM, which has hindered dissemination of the model beyond the research context. Determination of parameter values from experimental data is often not straightforward and this has hindered dissemination of the model among practitioners. The main difficulty is related to the calibration of the isotropic virgin response as individual aspects of soil behaviour are controlled in BBM by multiple parameters while a single parameter can control more than one aspect of soil behaviour. Consequently, iterative calibration procedures are common practice, where parameter values are adjusted in turn to match experiments. These procedures require significant experience, are time consuming and often lead to different parameter values.

Modified State-Surface Approach (MSSA)

A modified state surface approach (MSSA) was first proposed for investigating the mechanical behavior of unsaturated soils. It was then extended to study the coupled hydro-mechanical behavior of unsaturated soils with a special focus on the consistency between

different soil phases. However, hydraulic, and mechanical hysteresis were neglected in MSSA formulations. In their paper (Riad & Zhang, 2020a), based on evidence from experimental results, the MSSA is extended further to study the coupled hydro-mechanical hysteresis behavior of unsaturated soils. The extended MSSA can reproduce several forms of mechanical and hydraulic behavior observed in experimental results that cannot be represented by existing constitutive models. According to (Zhang & Lytton, 2009a), the MSSA represent unsaturated soil behavior under isotropic stress conditions in which a conventional void-ratio state surface is made up of an elastic surface and a plastic hardening surface. The plastic hardening surface always remains stationary, whereas the elastic surface remains unchanged when the soil experiences elastic deformation and moves downward when there is plastic hardening occurrence. Using the MSSA, the loading–collapse (LC) and the suction increase (SI) yield curves in the Barcelona basic model (BBM) are derived.

The paper by (Zhang & Lytton, 2009b) proposes a general theoretic formulation for the modified state-surface approach based on the theory proposed by Fredlund and co-workers. The signs and physical meanings of the material properties, the shapes of the loading–collapse (LC) and suction increase (SI) yield curves, and the mechanisms used in the Barcelona basic model (BBM) to model unsaturated soil behavior are discussed. Some other problems, such as stress-path independence and its implication on material properties, as well as coupling effects between the LC and SI curves, are also discussed. Based on analysis, it was found that with a minor modification, the modified state surface approach can be used to study both unsaturated expansive and collapsible soil behavior in a unified framework. (Riad & Zhang, 2020b)

Glasgow Coupled Model (GCM)

The coupled mechanical and water retention elasto-plastic constitutive model of Wheeler, Sharma and Buisson (the Glasgow coupled model, GCM) predicts unique unsaturated isotropic normal compression and unsaturated critical state planar surfaces for specific volume and degree of saturation when soil states are at the intersection of mechanical (M) and wetting retention (WR) yield surfaces. Experimental results from tests performed by Sivakumar on unsaturated samples of compacted speswhite kaolin confirm the existence

and form of these unique surfaces. The GCM provides consistent representation of transitions between saturated and unsaturated conditions, including the influence of retention hysteresis and the effect of plastic volumetric strains on retention behavior, and it gives unique expressions to predict saturation and de-saturation conditions (air-exclusion and air-entry points, respectively). Mechanical behavior is modelled consistently across these transitions, including appropriate variation of mechanical yield stress under both saturated and unsaturated conditions. The expressions defining the unsaturated isotropic normal compression planar surfaces for specific volume and degree of saturation are central to the development of a relatively straightforward methodology for determining values of all GCM parameters (soil constants and initial state) from a limited number of laboratory tests. This methodology is demonstrated by application to the experimental data of Sivakumar. Comparison of model simulations with experimental results for the full set of Sivakumar's isotropic loading stages demonstrates that the model can predict accurately the variation of both specific volume and degree of saturation during isotropic stress paths under saturated and unsaturated conditions. (Lloret-Cabot, Wheeler, & Sánchez, 2017)

2.1.3 Infiltration of Water into Soil Embankments

As cited by (Cho & Lee, 2001), for a fixed initial moisture content and rainfall intensity, the actual amount of rain that may infiltrate the ground at a given period ranges from zero to infiltration capacity. The greatest rate of water absorption by a particular soil is known as infiltration capacity; it varies over time and, as infiltration progresses, approaches a minimum value (about equal to saturated hydraulic conductivity). When rainfall intensity is less than the minimal infiltration capacity, all rainfall can infiltrate into the soil, according to Mein and Larson's phases of infiltration for uniform rainfall intensities. All rainfall also percolates into the soil when rainfall intensity is greater than the minimum infiltration capacity but does not exceed the soil infiltration capacity during the early phases of infiltration. The water that exceeds the infiltration capacity, however, runs off as runoff when the infiltration capacity falls below the intensity of the rainfall.

Several researchers (hydrogeologists, soil scientists, and geotechnical engineers) have examined the physical processes of rainwater infiltration into the ground and subsequent

seepage through the soil strata. Numerical models and equations have been created and developed for application. However, several significant restrictions on the application of these equations and models are explained in the paragraphs that follow. (Anderson & Pope, 1984) (Ng & Shi, 1998) (Lam, Fredlund, & Barbour, 1987) (Pradel & Raad, 1993)

During infiltration, the velocity of water in a porous material, qw, is given by Darcy's law which involves the coefficient of hydraulic conductivity and the gradient of potential (qw = kwsatrΨ). In addition, osmotic potential is null during infiltration because water infiltrates contain solutes so that there is no difference in osmotic pressure between rain and infiltrated water. This means that only the matric and the gravitational potential are involved in the infiltration process.

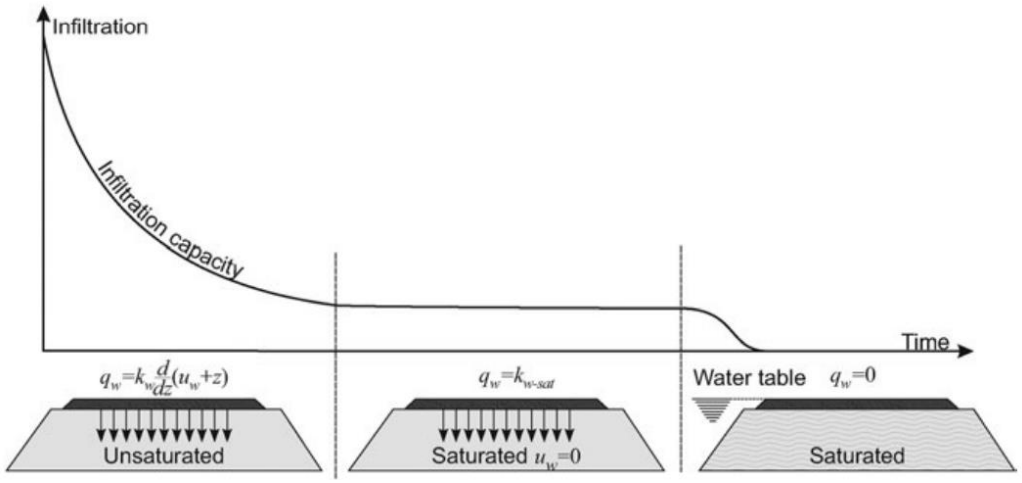

Figure 2 Different stages in the process of water infiltration

Figure 2 illustrates the following phases of water infiltration:

1. The gradient of potential is very high during the first stage of infiltration because of the high matric suction. In this stage the permeability of the porous material is low, but the effect of the high gradient of potential predominates and leads to a high velocity of infiltration. Afterward, the velocity of the water flowing through the surface decreases progressively as the surface of the porous material becomes wetter.

2. In the second stage of infiltration the porous material becomes saturated. If the water flows vertically without obstructions, the pore pressure becomes zero throughout the layer undergoing infiltration. Under this circumstance, the gradient of potential is one

because it involves only the gravitational potential, i = dz/dz = 1. Therefore, the velocity of infiltration is equal to saturated hydraulic conductivity, qw = kwsat.

3. In the last stage of infiltration, the flow of water may encounter one or more obstacles. Usually, these obstacles are layers of lower permeability. This situation increases the pore water pressure, raises the level of the water table, and reduces infiltration to zero. The velocity of water in these three phases can be computed by solving the set of equations and imposing a thin layer of water on the surface undergoing infiltration. In other words, the surface has an imposed water pressure of uw = 0

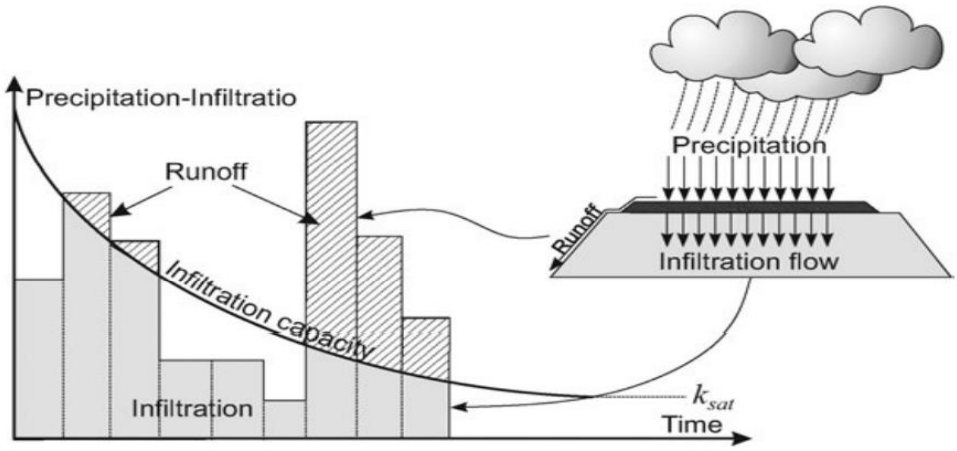

Figure 3 Assessment of the infiltration and runoff depending on infiltration capacity of the surface.

For a given volume of precipitation, the equilibrium between the infiltration capacity of the surface of the embankment and/or its surroundings is depicted in Figure 3.

Two cases are possible:

• The capacity of the surface to accept water is greater than the volume of rainfall from all sources of infiltration, in this case all the precipitation infiltrates.

• The volume of rain is greater than the capacity of the surface to soak up water. In this case the volume of water that infiltrates is given by the infiltration capacity, and the entire volume of water that exceeds this capacity becomes runoff.

2.2 Empirical Literature Review

2.2.1 IDF Curves for Addis Ababa

Addis Ababa has a pronounced rainfall peak during the boreal summer (July to September) and exhibits a rainfall minimum during the boreal winter (November to February). The city has a temperate climate due to its high-altitude location in the subtropics. Mean annual precipitation varies between 730 mm, considering historical data, and 980 mm, considering climate projections (Giugni et al. 2012).

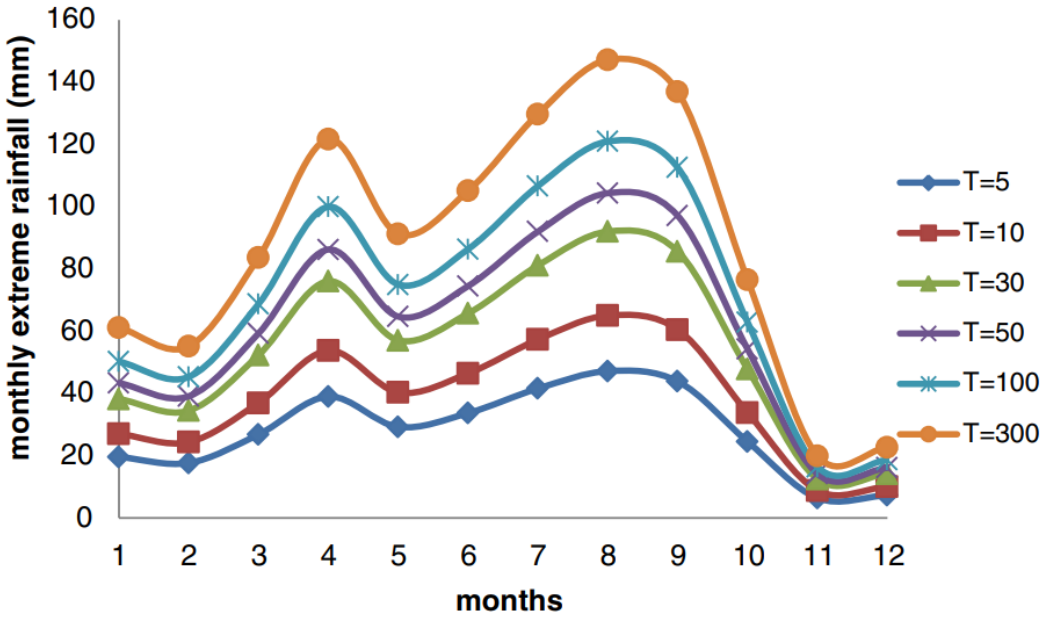

Figure 4 Variation of monthly extreme rainfall for different return period for Addis Ababa (using historical data and climate projections - scenario RCP 8.5)

In order to estimate the contingent influence of climate change on the IDF curves, the described procedure was applied to the climate (rainfall) simulations over the time period 2010–2050, provided by CMCC (Centro Euro-Mediterraneo sui Cambiamenti Climatici). The evaluation of the IDF curves allowed to frame the rainfall evolution of the three case studies, considering initially only historical data, then taking into account the climate projections, in order to verify the changes in rainfall patterns. The same set of data and projections was also used for evaluating the Probable Maximum Precipitation (PMP).

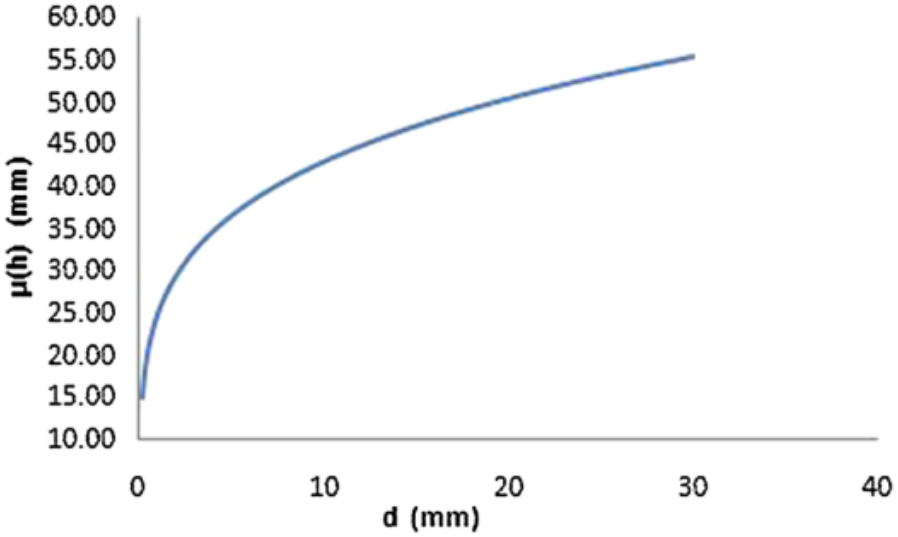

Figure 5 IDF curve for the city of Addis Ababa

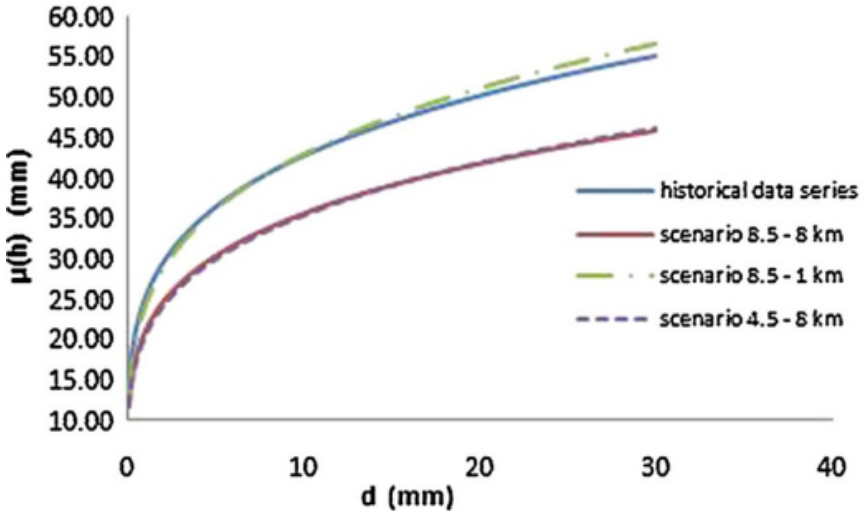

Figure 6 IDF curves for the city of Addis Ababa considering both historical data series and climate projections.

Table 1 Evaluation of PMP for Addis Ababa

	1964-2010							1964-2049						
t (min)	X_n (mm)	σ_n (mm)	X_M (mm)	$k_{m\ WMO}$	PMP WMO (mm)	k_m	PMP (mm)	X_n (mm)	σ_n (mm)	X_M (mm)	$k_{m\ WMO}$	PMP WMO (mm)	k_m	PMP (mm)
10	18.1	6.3	31.8	10.9	87.5	2.3	32.7	16.0	6.7	31.8	11.8	95.0	2.3	31.5
30	30.4	9.7	53.3	9.6	123.8	2.5	55.0	25.4	10.3	53.3	10.8	135.9	2.7	53.2
60	36.4	11.3	63.3	12.0	171.7	2.6	65.4	31.0	11.8	63.3	13.0	183.9	2.7	62.8
180	38.2	12.3	70.7	13.3	201.5	2.9	73.9	34.2	12.3	70.7	13.9	204.9	2.9	69.9
360	43.7	14.2	83.7	15.4	262.1	3.1	88.2	40.5	13.3	83.7	15.7	249.2	3.2	82.7
720	50.0	16.5	99.2	15.9	312.1	3.4	105.4	47.4	15.3	99.2	16.1	292.5	3.3	97.6
1440	52.5	18.1	110.0	17.6	370.5	3.6	118.4	54.4	20.0	120.3	17.5	404.2	3.2	117.5

Table 2 Evaluation of return period for the PMP values for the duration of 24 hours

		Historical data			Historical data + projections		
		k_m	PMP	T	k_m	PMP	T
Addis Ababa	*WMO*	17.57	370.48	1.E + 05	17.48	404.21	2.E + 05
	Evaluated	3.64	118.39	126	3.15	117.47	101
Dar Es Salaam	*WMO*	16.44	466.48	1.E + 05	17.23	576.38	1.E + 06
	Evaluated	3.30	156.63	157	3.13	154.00	237
Douala	*WMO*	13.22	863.15	4.E + 04	14.21	840.09	2.E + 04
	Evaluated	3.54	349.67	112	4.18	342.21	99

2.2.2 Red Clay Soils of Addis Ababa

Several investigation and characterization studies have been conducted on the Addis Ababa Red Clay. Their parent rocks are Olivine Basalt, Basalt, Trachyte. These soils have fair to good drainage. The principal clay minerals are Kaolinite, Hallysite, and Montmorillonite. Their PH value ranges between 5.1 and 6.8 according to (Lyon Associates Inc. & Building and Road Research Institute, 1971)

Medhanit Akalu of the School of Earth Sciences of Addis Ababa University has conducted an extensive study on the engineering characteristics of red soil in the western Addis Ababa. The engineering behavior of residual soils in the area, derived from the in-situ weathering and decomposition of parent rock has determined by certain physical characteristics designated as engineering properties. In this research work, some peculiar geotechnical and physio-chemical characteristics have been investigated on red soils from western Addis Ababa area. Laboratory test have also been conducted to characterize the soils. (Akalu, M., 2017)

Yodit Muluneh's study of 2012 is titled **"*Correlation between Critical State Soil Parameters and Index Properties of Remolded Red Clay Soils of Addis Ababa.*"** In this study, correlations have been developed to predict critical state soil parameters (CSSP) from index tests so that one can be able to model Addis Ababa red clay soils with critical state model using simple laboratory tests. Disturbed soil samples from six different sites of Addis Ababa, where red clay is found, are collected. Laboratory tests like specific gravity, grain size analysis, Atterberg limit and standard compaction for a total of twelve test samples (at 1.5m and 3.0m depths per each six sites) are conducted. By remolding these samples to maximum dry

density (MDD) and optimum moisture content (OMC), twelve - one dimensional consolidation and six- isotropic consolidation triaxial tests have been done. From these tests critical state soil parameters (λ and Γ) are determined. From the results of limited tests, an indicative good correlation is observed between (Γ and LL), (Γ and, PL), (Γ and PI), (λ and LL) and (λ and PL). But poor correlation is developed between λ and PI. (Muluneh, Y., 2012)

A summary of results on physical properties of AARC from these studies has been presented in the following table.

Table 3 Summary of physical properties of AARC

Physical Behavior	Morin and Parry (1971)	MERIHUN LUKAS (2010) (2.5 m)				Yodit Muluneh (2012)				MEDHANIT AKALU (2017)
		Addisu Gebeya		Kolfe		Addisu Gebeya		Kolfe		
		1	2	1	2	1.5 m	3.0 m	1.5 m	3.0 m	
ω (%)	-	27	28	22	27	-	-	-	-	14 – 59
Gs (-)	2.61-2.91	2.71	2.73	2.72	2.73	2.73	2.72	2.66	2.74	2.6 – 2.8
ρ_{bulk} (g/cm^3)	-	1.90	1.90	1.92	1.87	-	-	-	-	-
P_{wet} (g/cm^3)	-	1.83	1.86	1.95	1.78	-	-	-	-	-
P_{200} (%)	34 - 76					-	65.69	-	76.55	-
SL (%)	10-30	17	20	12	17	-	-	-	-	-
LL (%)	44 - 66	63	72	61	71	59	59	62	63	39 – 106
PL (%)	-	28	33	27	33	31	30	39	40	-
PI (%)	14 - 30	35	39	34	38	28	29	23	23	9 – 40
A (-)	-	-	-	-	-	-	-	-	-	0.11 – 0.70
SF (%)	-	32.5	33.0	10.0	20.0	-	-	-	-	5 – 80
MDD (g/cc)	1.18 - 1.69	1.37	1.39	1.53	1.36	1.58	1.58	1.55	1.52	1.25 – 1.64
OMC (%)	38 - 29	34	34	28	32	25.0	25.0	24.3	26.3	19 – 34
UCS (kPa)	147-251	-	-	-	-	-	-	-	-	64 – 213

"A Study on Shear Strength Characteristics of Addis Ababa Red Clay Soil for Unsaturated Case" is the title of a research work conducted in 2010 by Getaneh W/Medhin. He has undertaken this study with the objective of investigating the shear strength characteristics of Addis Ababa red clay soils for unsaturated case using the modified triaxial testing machine which allows the independent measurement of pore-air and pore water pressures and to compare it with the results obtained for saturated soil samples. (W/Medhin, G., 2010)

A summary of results on mechanical properties of AARC from these studies has been presented in the following table.

Table 4 Summary of results on mechanical properties of AARC

Mechanical Behavior		Merihun Lukas (2010) (2.5 m depth)				Yodit Muluneh (2012)				Medhanit Akalu (2017)
Behavior	Parameter	Addisu Gebeya		Kolfe		Addisu Gebeya		Kolfe		
		1	2	1	2	1.5 m	3.0 m	1.5 m	3.0 m	
Compressibility	C_c (-)	0.152	0.172	0.147	0.195	0.199	0.191	0.199	0.186	0.124 - 0.330
	P_c (kPa)	380	280	340	380	-	60	-	75	-
	OCR (-)	8.2	6.0	7.2	8.2	-	-	-	-	-
Shear Strength	C' (kPa)	20.0	15.3	23.4	23.0	-	-	-	-	6 – 63
	Φ' (deg)	15.5	21.3	16.7	19.2	-	-	-	-	11 – 34
	λ (-)	-	-	-	-	-	0.0856	-	0.1036	-
	Γ(κ?) (-)	-	-	-	-	-	2.2503	-	2.3718	-

Nuru Ismail (2013) has conducted a study under the title ***"Prediction of Soil Water Characteristic Curve Based on GSD and PI for Red Clay and Expansive Soils Found in Addis Ababa"*** as his master's thesis theme at Addis Ababa Institute of Technology in 2013. His work included prediction of soil water characteristic curve (SWCC) and unsaturated shear strength parameter, Φb of Addis Ababa soils based on Atterberg limit tests, free swell tests, grain size distribution analysis outputs etc (Ismail, N., 2013). Moreover, a suction controlled triaxial testing was conducted by (W/Medhin, 2010) whose key results are summarized in the table below.

Table 5 Modified Triaxial with Controlled Suction

Site	Pit	Depth	Sample no.	σ'_3	(Ua-Uw)	$(\sigma'_1-\sigma'_3)_f$	C'	C	$(Ua-Uw)_f$	ϕ'	ϕ^b
		(m)		(kPa)	(kPa)	(kPa)	(kPa)	(kPa)	(kPa)	(deg)	(deg)
Kolfe	1	2.5	Saturated	250	0	315.2					
			1	250	30	340.5	36.19	41.90	16.75	21.00	18.80
			2	250	50	392.2		50.67	36.60		21.55
			3	250	70	429.8		56.70	50.20		22.22
	2	2.5	Saturated	150	0	188					
			1	150	30	247.8	25.00	28.83	21.50	20.99	20.10
			2	150	50	296.8		39.67	42.80		23.60
			3	150	70	339.9		46.67	52.90		25.87

2.2.3 Influence of Matric Suction Variation on the Performance of Railway Embankments

Because of their exposure to climate change, earth constructions such as embankments are exposed to seasonal fluctuations in water content. Climate actions are cyclical, which could lead to accumulating deformations. Because of the cyclic nature of service loads, railway embankments require constant maintenance; yet, if the infrastructure lacks adequate drainage systems, the mechanical qualities of the infrastructure may deteriorate rapidly due to climatic exposure. (R Cardaso, 2015)

There are several studies described in the literature on the effects of suction cycles in the mechanical properties of compacted soils ((e.g. Cui and Delage, 1996; Lloret et al., 2003; Zhan and Ng, 2006)) but very few consider the effects of cumulative wetting and drying cycles in their hydro-mechanical behavior. For the particular case of railway embankments, the degradation of the mechanical properties of the foundation layers of the track (the track bed) may increase significantly due to climate exposition, in particular if the infrastructure has no efficient impervious and drainage systems (López Pita et al., 2007). Adding to this, seasonal displacements caused by soil-atmosphere interaction may result in accumulated deformations. (Vahedifard & Robinson, 2015)

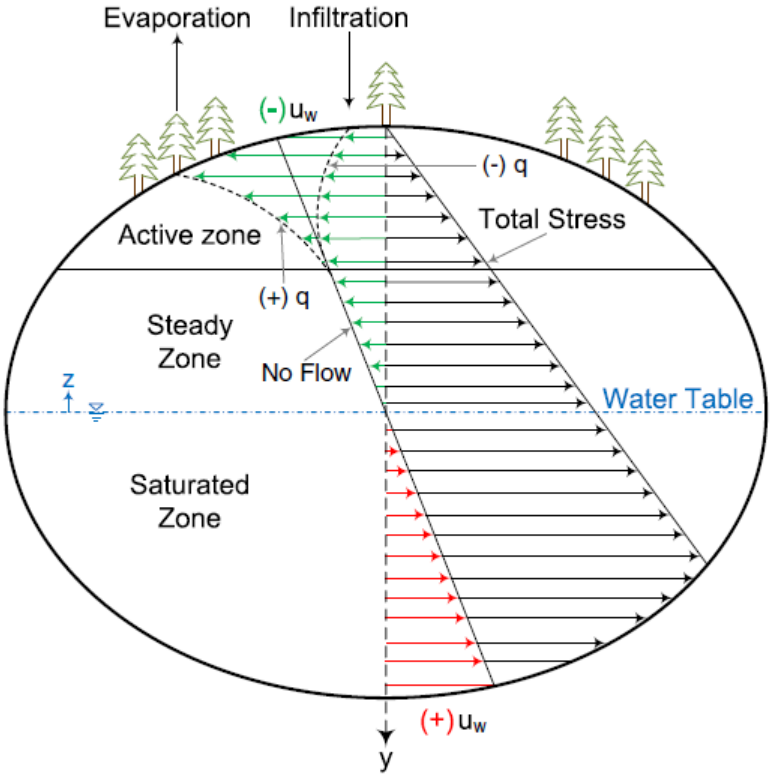

Figure 7 Matric suction profiles under various surface flux boundary conditions (adapted from Fredlund 1996)

Concerning the performance of the railway infrastructure, an adequate characterization of seasonal displacements may help to design solutions with reduced maintenance needs. Seasonal fluctuations in water content are usually limited to shallow depth, according to several studies, and correspond to alternate wetting and drying. (Y.J. Cui, 2010) However, few research indicate that the influence depth of soil-atmosphere interaction is limited for volumetric water content, but it is much greater for temperature and can occur up to large depths. (Ni An, 2017)

Several studies are also conducted on the effect of suction cycles on the mechanical properties of compacted soils. Trinh et al. (2012) conducted a series of cyclic tests on the fouled ballast in ancient railway track substructure, and the results suggested that the lower moisture contents in samples led to higher shear strength and lower permanent strain. (Oh, Vanapalli, Qi, & Han, 2016) Test results revealed that the increase of matric suction could increase shear modulus and decrease the damping ratio. (Rafaela Cardoso, 2007)

The drying-wetting effect and the suction history of railway embankment materials may have a considerable effect on its mechanical behavior under the expected loads. There are not many researchers conducted to study the effects of suction history on the mechanical behavior of railway embankment materials. Testing on clay and silt through the regular size triaxial test apparatus have shown that the suction and suction history have significant effects on the resilient modulus and the permanent strain of the soil. (Zhigang Cao, 2020) However, the influence of the suction history on the mechanical behavior of the railway embankment materials remains unclear. Therefore, it is necessary to investigate the effects of suction history on the mechanical behavior of the railway embankment to grasp a deep understanding of the long-term performance of the railroad. (A. S. O'Brien, 2004)

2.3 Conceptual Framework

As highlighted in the previous part of this literature review section, there is a gap in literature regarding the effect of seasonal changes in suction on behavior of railway embankments in Ethiopia. To address this issue, a conceptual framework presented in Figure 8 is utilized.

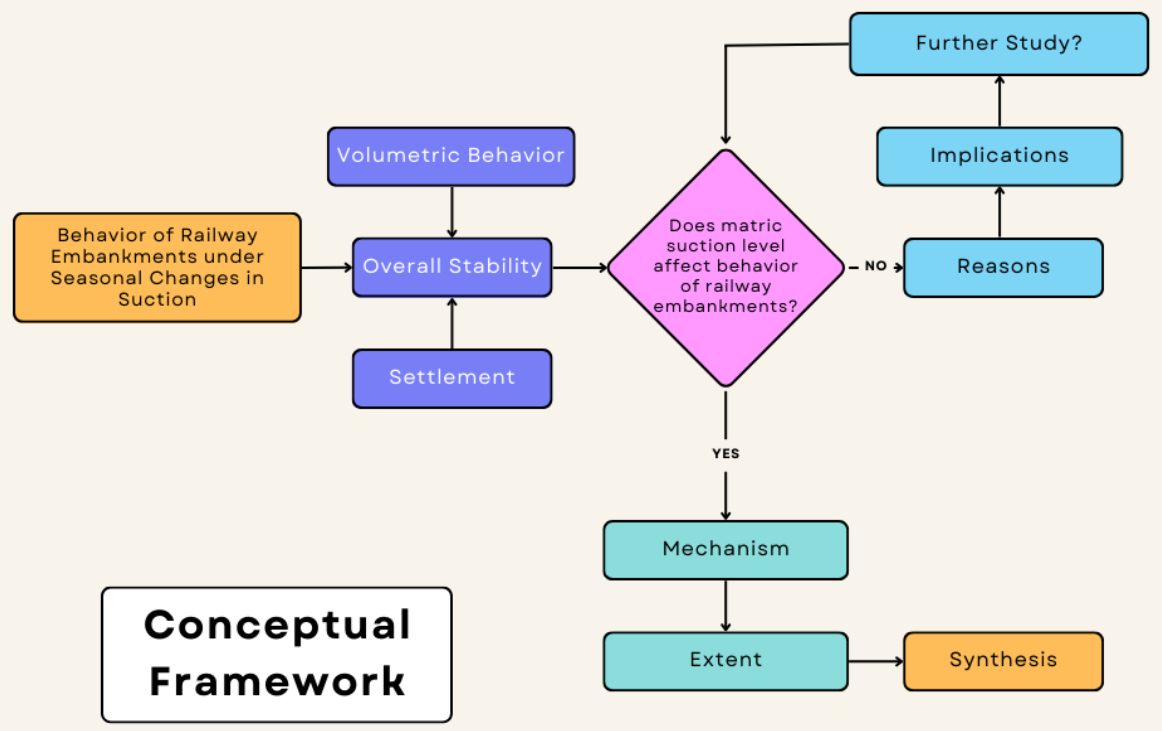

Figure 8 Conceptual Framework

3. Research Methodology

3.1 Research Design

The research design adopted for this specific project is experimental design setting which provides a certain degree of control over the factors that may affect the dependent variable(s) being studied. In this case the effect of matric suction cycle on mechanical performance of an embankment is being studied.

A desktop study of relevant literature and data has been conducted. A compacted red clay used as embankment material in Addis Ababa LRT northern most section is the subject of this study. All relevant literature on the red clay soils of Addis Ababa has been assessed. The site for data collection is selected based on convenience for sample retrieval.

3.2 Data Collection / Generation

A soil sample has been collected from Addisu Gebeya area which is known to be an area of red clay soil prevalence. The sample has been collected at a depth of 5 m from NGL in this site and has been used in the analysis of the "At-Grade Embankment". A soil sample also has been collected from 5 kilo area at a depth of 15 m whose behavior has been utilized as an input in the analysis of the embankment section with extension of AARC natural ground.

Table 6 Testing program.

Test	Testing Material	Apparatus	Remarks
Grainsize Distribution	Natural ground	Sieve + Hydrometer	6
Atterberg Limits	Natural ground	Casagrande	6
Permeability	Subgrade clay	Permeameter	6
Strength	Natural ground	Triaxial Tests	2
Stiffness	Natural ground	Oedometer	2
Compaction	Subgrade clay	Standard Proctor	6

3.3 Data Analysis

3.3.1 Climate Data Analysis

A data set for the City of Addis Ababa is acquired from Ethiopian Meteorology Agency (EMA) for the period 1980 – 2020. Annual maximum precipitation series has been extracted from the dataset for 15 minutes to 10 days duration after going through the initial screening process. The series is then used in Regional Frequency Analysis (RFA).

The temporal downscaling method employed in this study is a modified version of a stochastic method introduced by (Scott Socolofsky, 2001). They used the method to downscale daily precipitation data to hourly data. The method developed for this project breaks 3-hourly precipitation into possible storm intensity patterns by selecting samples of measured event statistics from a 15-min observed precipitation data (Scott Socolofsky, 2001).

3.3.2 Infiltration Analysis

To model the infiltration phases of rainfall, flux was controlled at the slope surface as a boundary condition. For example, the Surface flux can be used to define the ground surface boundary conditions when the rainfall intensity on the ground surface is inputted. This function applies a forced inflow rate, as large as the rainfall intensity, onto the ground surface. If the absorption capability of the soil stratum surface is larger than the rainfall intensity, the soil stratum absorbs all the rainwater. However, if the absorption capability is smaller, rain is absorbed into the ground surface by only the absorption capability amount, and the rest of the rain flows across the ground surface. If the rainfall intensity is larger than the absorption capability, the ground surface is in a saturated state during rainfall, as if the groundwater level existed above the surface. Hence, the area of rainfall needs to be changed to a water level line.

3.3.3 Numerical Analysis

The performance in service of a railway embankment is simulated MIDAS software. Climate data considered corresponds to average annual distributions of precipitation, relative humidity and temperature. Stability analysis and settlement computation have taken place.

Strength Reduction Method (SRM): Nonlinear FEM-coupled strength reduction method which gradually decreases the shear strength and friction angle until the calculation does not converge, and that point is considered to be the failure point of the slope. The maximum strength reduction ratio at that point is used to calculate the minimum safety factor of the slope. Both Elastic Settlement and Consolidation Settlement have been computed for the embankment.

MIDAS **GTS NX** is finite element analysis software for advanced geotechnical analysis of soil and rock deformation and stability, as well as groundwater flow. GTS NX is used for analysis, testing, and design by geotechnical, civil, and mining engineers. It is designed to adapt any kind of geotechnical project. The intuitive interface will enable new users to easily integrate the software in their work process. The fast analysis speed, outstanding graphics, and output capabilities will provide users with a new and advanced level of geotechnical design.

In addition to the availability of the genuine software, the following four points summarize why I chose the software for my research.

- ✓ Real 3D Geometry Modelling
- ✓ Powerful Mesh Generator
- ✓ Fast Analysis Solver
- ✓ Outstanding Post-Processing

3.4 Presentation of Results

Results of slope stability have been presented and discussed in terms of both short term and long-term stability. In addition to that, results of settlement computation have been presented. Also, different conditions of saturation level of the embankment have considered and analyzed to consider the effect of matric suction.

4. Results and Discussions

4.1 Updated IDF of Addis Ababa City

IDF curves the observed and anticipated increasing trends in extreme rainfall magnitude and frequency, as well as the associated geohazards in the city of Addis highlighted the need for revising and updating the local intensity-duration-frequency (IDF) curves. Increased storm frequency and intensity related to climate change are exacerbated by such local factors as the growing occupation of floodplains, increased runoff from hard surfaces, inadequate waste management and silted up drainage.

In this study, the researcher set out to develop new and forward-looking rainfall and runoff IDF curves for Addis Ababa city using recently observed and projected precipitation and watershed data. Regional frequency analysis coupled with Bayesian uncertainty quantification and model averaging methods have been used to develop and update the rainfall IDF curves, which are then used in hydrologic model to develop the runoff IDF curves that explicitly account for effects of climate change into the IDF curves and related designs. This study aimed to develop IDF curves under the future climate scenarios for Addis Ababa, which have been compared with the IDF curves under the current climate.

Available rainfall records from Ethiopian Meteorological Agency are limited to daily time steps. Since rainfall data at shorter time steps are essential for the evaluation of IDF curves, a daily rainfall disaggregation model shall be adopted. The estimation and use of IDF curves rely on the hypothesis of rainfall series stationarity, namely that intensities and frequencies of extreme hydrological events remain unchanged over time. The available data concerns only the maximum daily data for a specified year of observation. To define the extreme values in a smaller time window (10', 30', 1 h, 3 h, 6 h, 12 h), a synthetic sequence of rainfall has been generated, with statistical properties equal to those of the observed rainfall. In greater detail, the daily rainfalls have been successively disaggregated using two models:

- cascade-based disaggregation model
- short-time intensity disaggregation method

Assuming that daily rainfalls derive from a marked Poisson process, i.e., rainfall lag and heights drawn from exponential probability density functions (whose parameters are calculated from observed rainfall series), it is possible to use a simple stochastic model of daily rainfall, that describes the occurrence of rainfall as a compound Poisson process with frequency of events λ. The distribution of times τ between precipitation events is an exponential with mean 1/λ, and exponentially distributed rainfall amounts h with mean γ.

A data consistency test has been conducted to detect any outliers in the data set.

Table 7 Data Consistency Test for Rainfall Data

S. No.	Year	Max. Prec.	LOG (RF)
1	1980	36.3	1.559906
2	1981	58	1.763428
3	1982	41.4	1.617000
4	1983	50.1	1.699837
5	1984	55.4	1.743509
6	1985	43.2	1.635483
7	1986	83.8	1.923244
8	1987	56.8	1.754348
9	1988	35.5	1.550228
10	1989	49.2	1.691965
11	1990	39.6	1.597695
12	1991	47.3	1.674861
13	1992	51.4	1.710963
14	1993	53.5	1.728353
15	1994	57	1.755874
16	1995	85.3	1.930949
17	1996	67	1.826074
18	1997	46.3	1.665581
19	1998	78.3	1.893761
20	1999	37.4	1.572871
21	2000	85.3	1.930949
22	2001	96.3	1.983626
23	2002	29.5	1.469822
24	2003	54.9	1.739572
25	2004	44.2	1.645422
26	2005	58.6	1.767897
27	2006	70.9	1.850646
28	2007	64	1.806180
29	2008	53.3	1.726727
30	2009	54.7	1.737987
31	2010	44.6	1.649334
32	2011	55.8	1.746634
33	2012	36.4	1.561101
34	2013	47.2	1.673942
35	2014	65.4	1.815577
36	2015	47.8	1.679427
37	2016	47.7	1.678518
38	2017	55.2	1.741939
39	2018	23.5	1.371067
40	2019	52	1.716003
41	2020	46.9	1.671172
42	2021	54.2	1.733999
43	2022	25.4	1.404833
	Average	55.32	1.7226132
	St. Dev.	17.85105	0.133802
	Skew	0.8798479	0.315509
	KN (43 YEAR)	2.71	2.71
XH (Higher threshold)		2.0852169	121.679350
XL (Lower threshold)		1.3600095	22.909179
Remark: There are no outliers			

As can be seen from Table 7, the data set is relatively consistent with no outlier detected.

Two methods have been employed to generate the updated IDF curves namely Gumble and Log Pearson III. The resulting curves are presented below in Figure 9 and Figure 10.

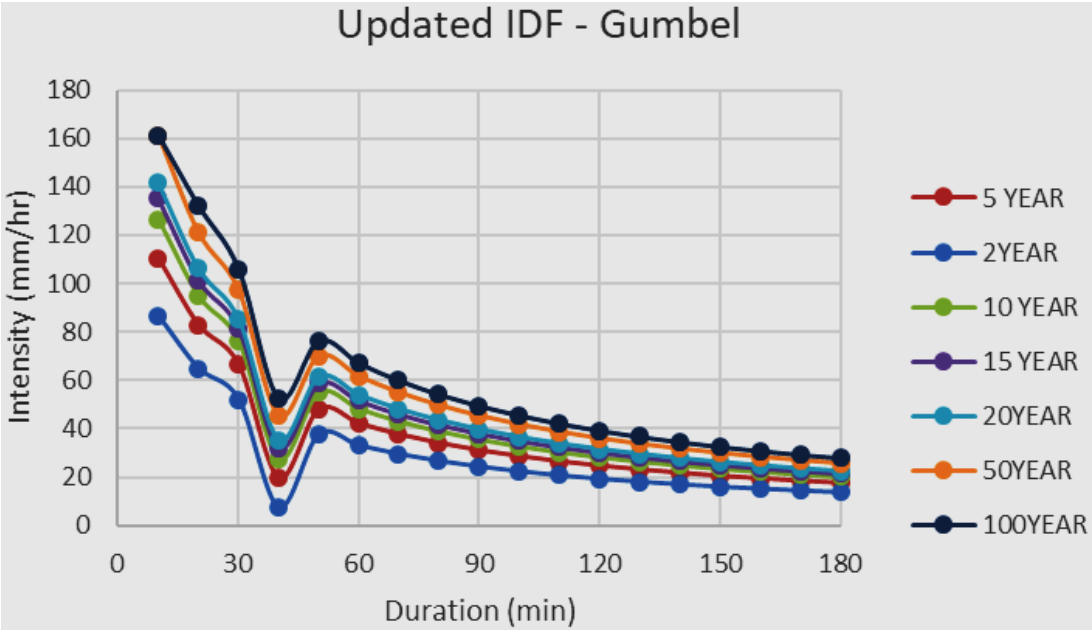

Figure 9 Updated IDF for AA City using Gumble Distribution

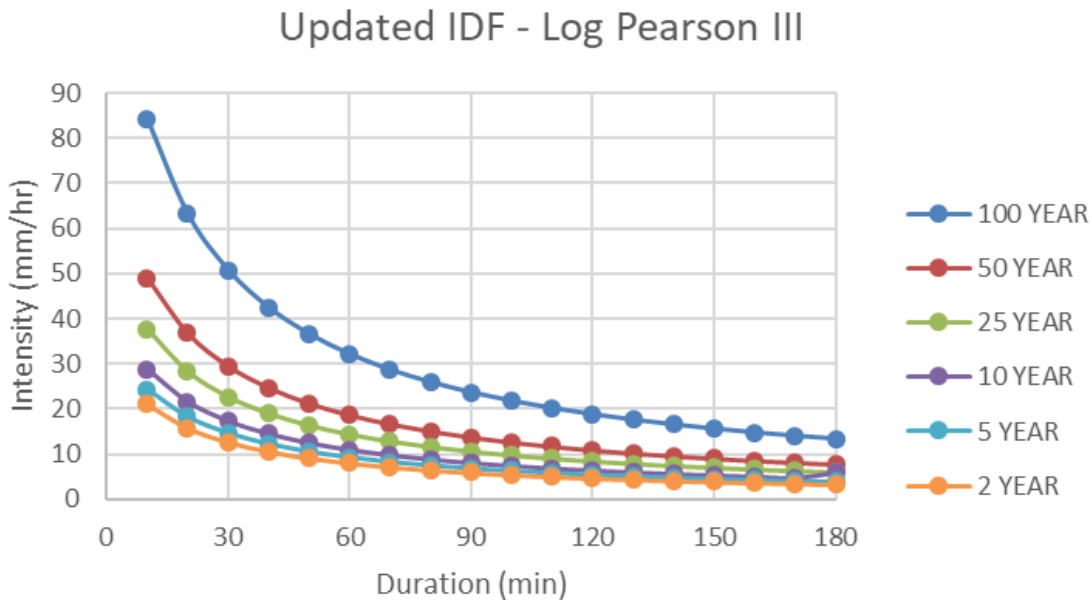

Figure 10 Updated IDF for AA City using Log Pearson III Distribution

As can be seen from Figure 9 and Figure 10, the 100-year return period precipitation produces the worst-case scenario.

4.2 Validation

The research chosen for the software validation is titled "Slope Stability Analysis of Unsaturated Soil with Fully Coupled Flow-Deformation Analysis" by Indra Noer Hamdhan and Helmut F. Schweiger. It was chosen because it highly resembles the current study in its objectives and sought after results. Slope stability analysis of unsaturated soil requires simultaneously compute deformation and groundwater flow with time dependent boundary conditions (fully coupled flow-deformation analysis).

A simple case of a homogeneous slope has been chosen. The international soil classification system USDA series is used for determining the hydraulic data for the analysis. The mechanical and hydraulic models used in the analysis are the Mohr Coulomb failure criterion and the Van Genuchten model respectively. Table 8 shows the hydraulic data used. The analysis was performed by utilizing the finite element code PLAXIS. The fitting parameters g_a is reciprocal of air-entry value, g_n controls the shape of the SWCC plot after the air-entry value, and g_l is a fitting parameter controlling the shape of the hydraulic conductivity plot.

Table 8 Hydraulic data used in model verification.

Soil	**K_{sat} (m/s)**	**g_a (1/m)**	**g_n (-)**	**g_l (-)**
Clay	5.5E-07	0.80	1.09	0.50

The height of the slope is 10 m, and the gradient (horizontal to vertical) is 2:1. Figure 11 shows the geometry and the two-dimensional finite element mesh consisting of 4800 15-noded elements.

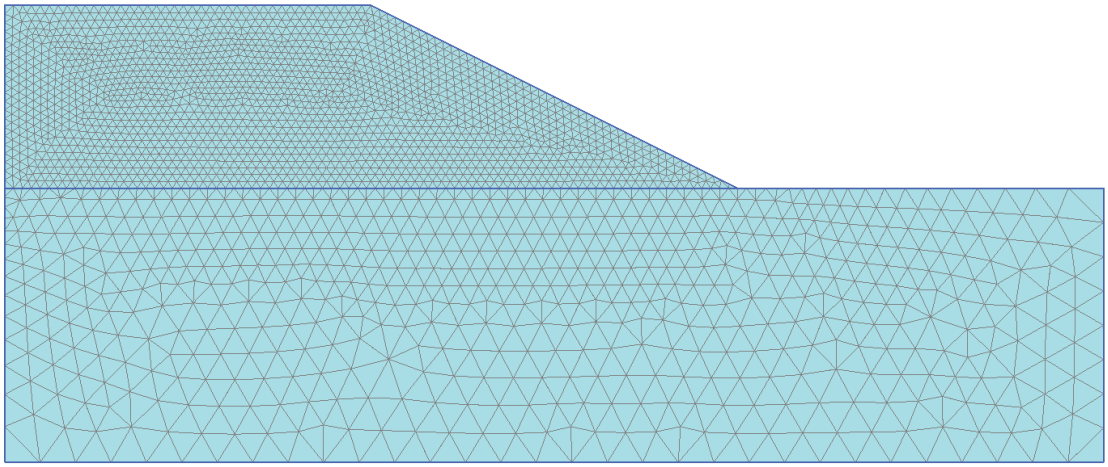

Figure 11 Geometry and finite element mesh of the slope.

For simplicity it is assumed that all the soils have the same shear strength and stiffness parameters. Soil parameters for the Mohr Coulomb model used in the analysis are given in Table 9.

Table 9 Soil parameters used in model verification.

Description	Symbol	Unit	Value
Unit weight	γ	kN/m3	20
Elasticity modulus	E'	kPa	7500
Effective Poisson's ratio	ν'	-	0.35
Effective cohesion	c'	kPa	20
Effective friction angle	ϕ'	deg	20

The initial ground water level was assumed to be horizontal at the level of the toe of the slope. A rainfall with intensity of 10 mm/hour lasting 3 days (72 hours) was applied on the crest and the slope. The minimum and the maximum pore pressure head respectively are -0.1 m and 0.1m. This means that water can flow on the surface with a maximum height of 0.1 meters. The left boundary, right boundary and lower boundary of the model were assumed impervious boundaries.

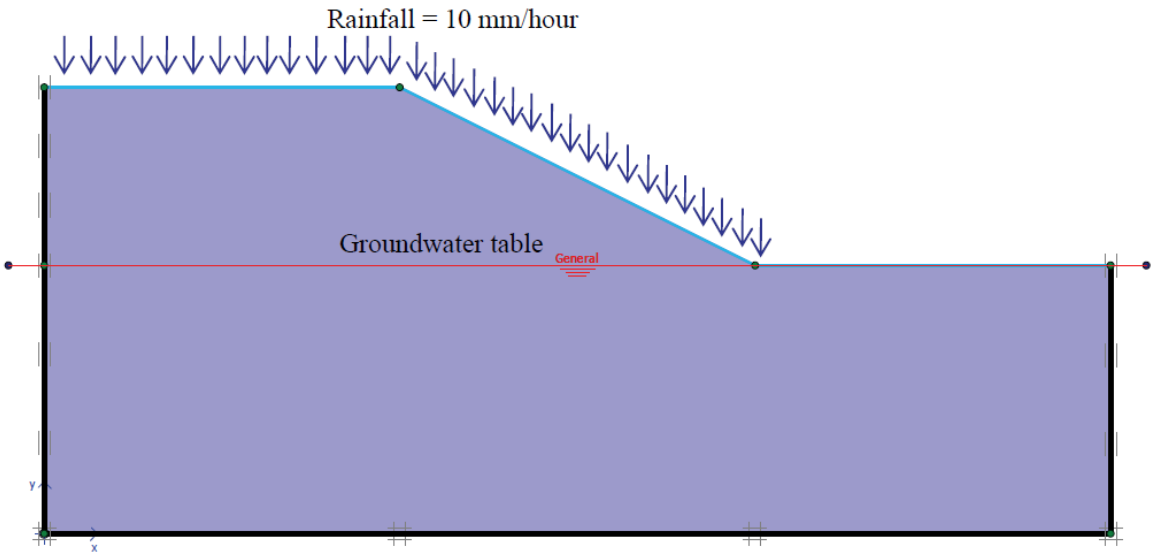

Figure 12 Boundary conditions used in the model validation.

The slope stability analysis results from the original research and the current study are presented side by side as follows.

Table 10 FoS from the original research and current study

Time (hours)	FOS	
	Original Research	Current Study
0	1.709	1.718
3	1.708	1.707
6	1.708	1.703
9	1.707	1.694
12	1.706	1.689
18	1.704	1.686
24	1.702	1.684
36	1.702	1.682
48	1.698	1.679
60	1.694	1.674
72	1.690	1.670

As can be seen from Table 10 and Figure 13, the results of the original research and current study are fairly consistent. The validation results show that no programming errors are identified in the computer code used for this analysis.

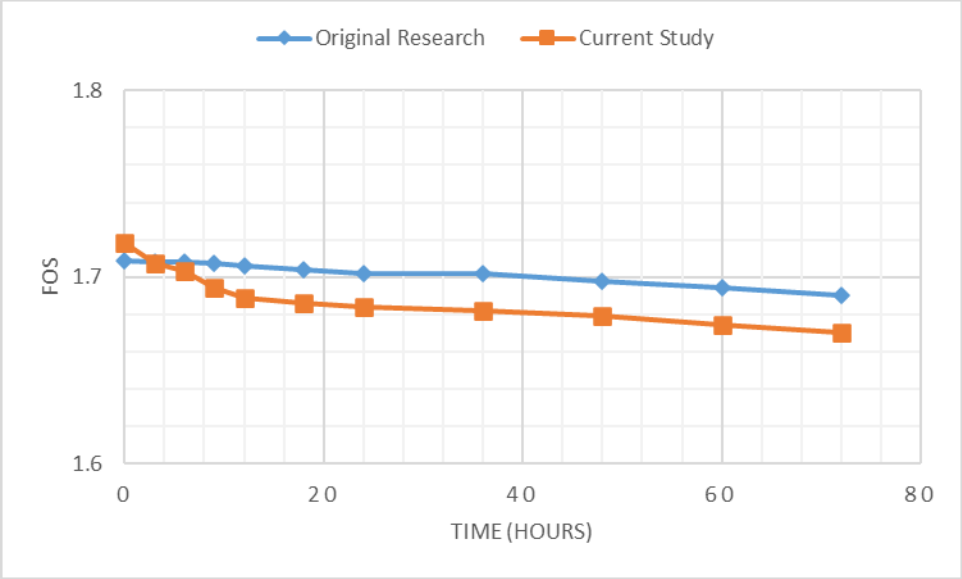

Figure 13 Plot of FOS from the two studies

4.3 Analysis Inputs

The following are some of the data required to carry out the analysis:

- Geometric data,
- Geotechnical data: SWCC, shear strength and permeability parameters for both saturated and unsaturated conditions
- Climatic data

The actual data used for the analysis are presented in the following sections.

4.3.1 Geometry and Finite Element Mesh

Figure 14 and Figure 15 present the geometric cross-section used in the analysis. The first one represents a section just outside the starting station at St. George Church whereas the later represents a section near the end of the North – South LRT line.

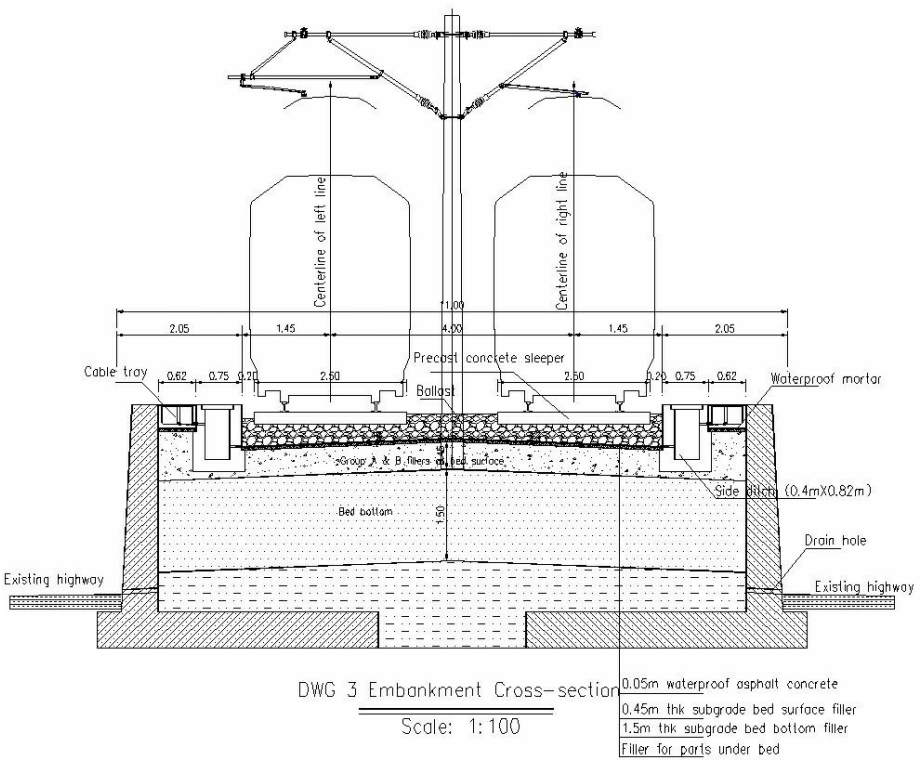

Figure 14 Geometry of a Typical Cross-section of the Embankment

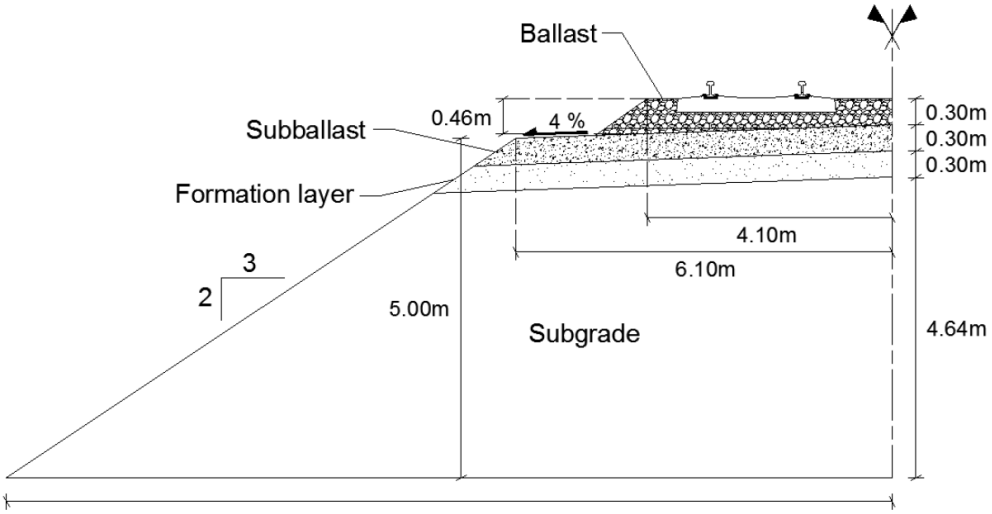

Figure 15 Geometry of the Cross-section of the Embankment considered for Analysis.

As can be seen from Figure 15, a finer mesh has been provided near the loads and slope boundaries to arrive at a better analysis result.

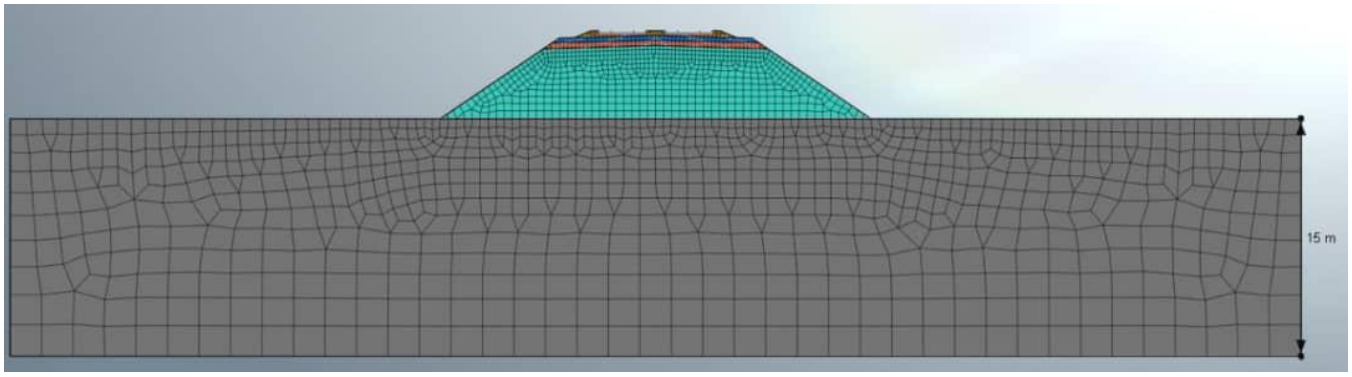

Figure 16 Model extent and meshing

4.3.2 Material and Interface Properties

Material Properties

Figures 14 and 15 present the SWCC of the red clay soil as measured by (Woto & Azmatch, 2022) using filter paper test. A summary of the index properties and shear strength and permeability parameters is presented in Table 8.

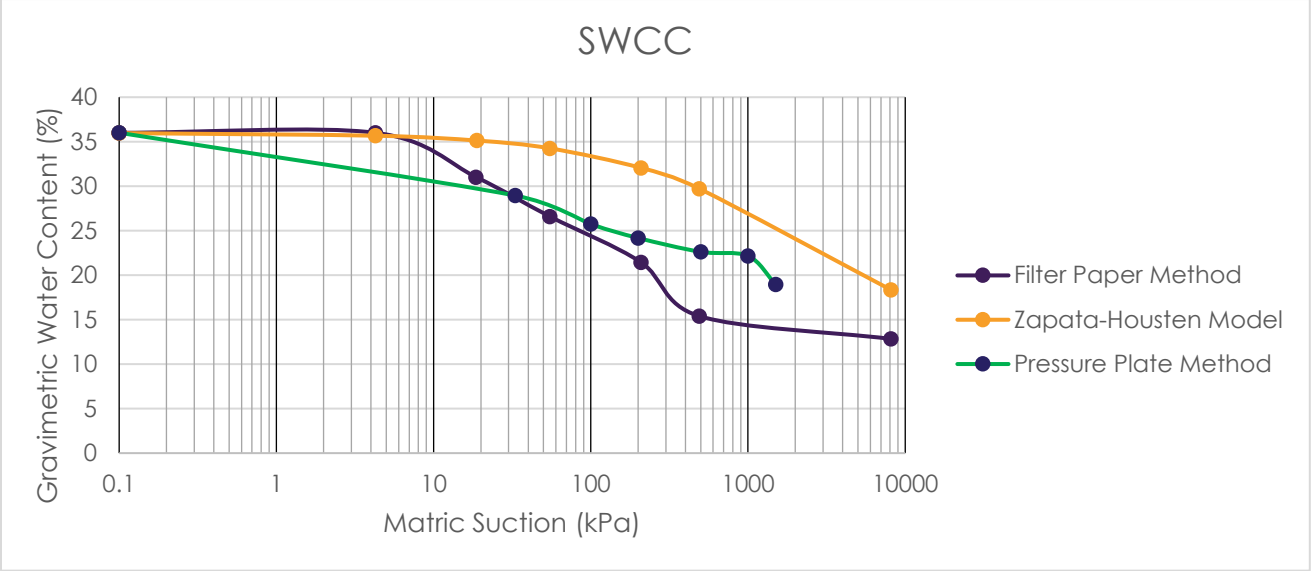

Figure 17 SWCC Curve for Red Clay Soil around Addisu Gebeya (Adopted from Sinishaw et.al)

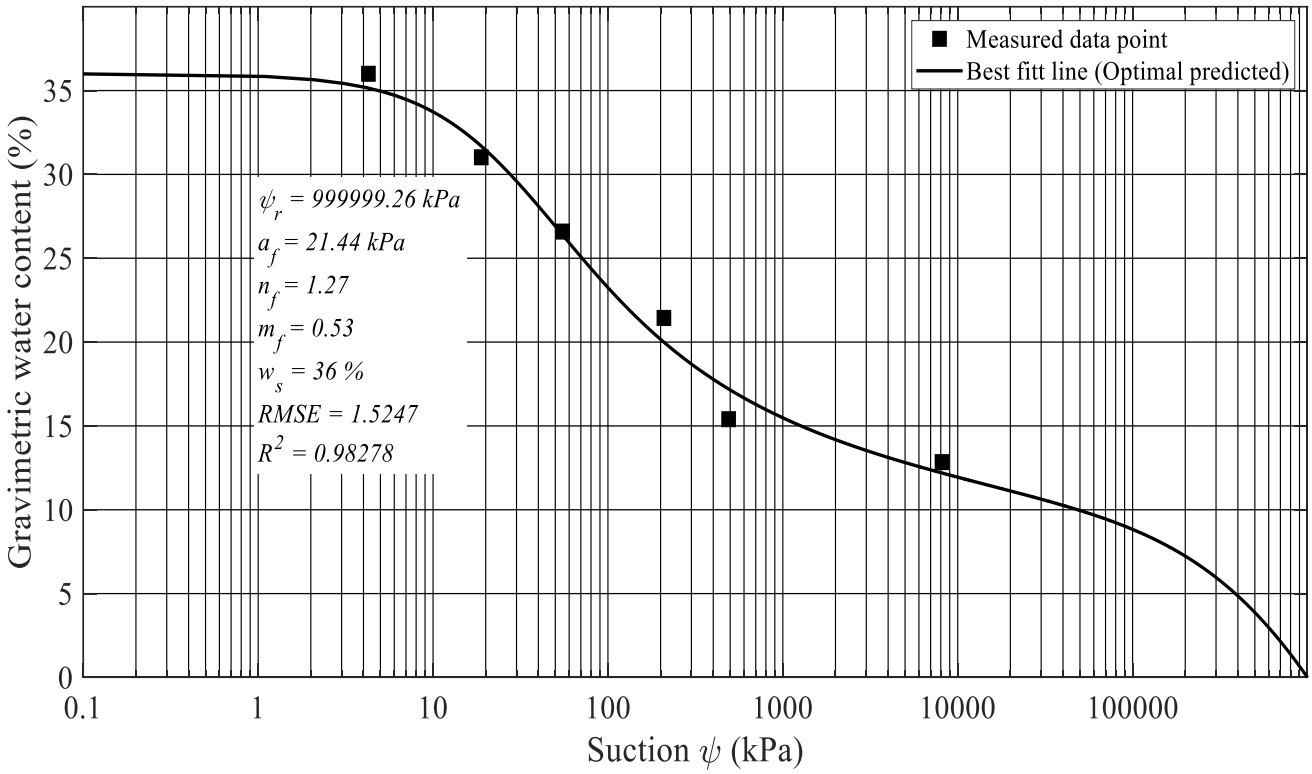

Figure 18 SWCC Curve for Red Clay Soil around 5 Kilo (Adopted from Sinishaw et.al)

Table 11 Strength and *Stiffness Parameters* used in the Model.

Parameters	Natural Ground		Compacted Embankment	Ballast Layer
	At 5 m depth	At 15 m depth		
Unit weight (kN/m^3)	19.00	20.00	18.25	15.30
Saturated hydraulic conductivity, k_s (m/sec)	3.17E-10	3.17E-10	9.5 E-11	N/A
SWCC parameter a, (kPa)	21.23	21.23	21.44	N/A
SWCC parameter n	1.2	1.2	1.27	N/A
SWCC parameter, m	0.55	0.55	0.53	N/A
Total Cohesion, c (kPa)	25.00	35.00	52.08	3
Total Friction Angle, ϕ (deg)	5	15	21.54	45
Effective Cohesion, c'(kPa)	20	21.3	41.87	1
Effective Friction Angle, ϕ' (deg)	15.3	15.5	14.11	40
Preconsolidation Pressure, Pc (kPa)	280	380	N/A	N/A
Compression Index, Cc	0.195	0.147	0.172	N/A
Creep Coefficient, Cα	0.0043	0.0034	0.003213	N/A
Over Consolidation Ratio, OCR	6.0	8.2	N/A	N/A
Young's Modulus (MPa)	30	70	100	200
Poisson's Ratio	0.35	0.4	0.30	0.30

Table 12 presents the material properties used for rails, sleepers as adopted from (Buddhima Indraratna, 2017)

Table 12 Material properties used for rails and sleepers.

Parameters	Rails	Sleepers
Density (kg/m^3)	2000	2000
Young's Modulus (MPa)	500,000	30,000
Poisson's Ratio	0.30	0.25

Interface Properties

Interface elements account for normal and shear directional relative displacement and interface traction that simulate face/face and line/line behavior. GTS NX divides Interface elements into line Interface elements and plane Interface elements. Line Interface elements are often used to simulate behavior between planar elements (Plane stress, Plane strain) in this case the boundaries between the ballast, sub ballast, subgrade, and natural ground. Plane Interface elements are often used to simulate behavior between solid elements or

between planar elements and solid elements, in this case between the rails, sleepers and ballast. Values adopted from (Buddhima Indraratna, 2017) and (Armen Ter-Martirosyan, 2019) have been utilized.

Table 13 Interface properties

Parameters	Interfaces elements
Normal properties	Hard contact
Tangential coefficients	0.450
Strength reduction factor	0.67

4.3.3 Loads and Boundary Conditions

The load used in the analysis are all adopted from AREMA manual, and they are summarized in Table 14. (American Railway Engineering and Maintenance-of-Way Association, 2019)

Table 14 Summary of loads considered.

Item	Load Value	Category	Type
Ballast	0.3 m * 19 kN/m^3 = 5.7 kN/m	Dead	UDL
Sleeper	2.4 kN/m	Dead	UDL
Track Rail	3 kN	Dead	PL
Wagon	Cooper E-80 Loading = 120 KN/m	Live	PL

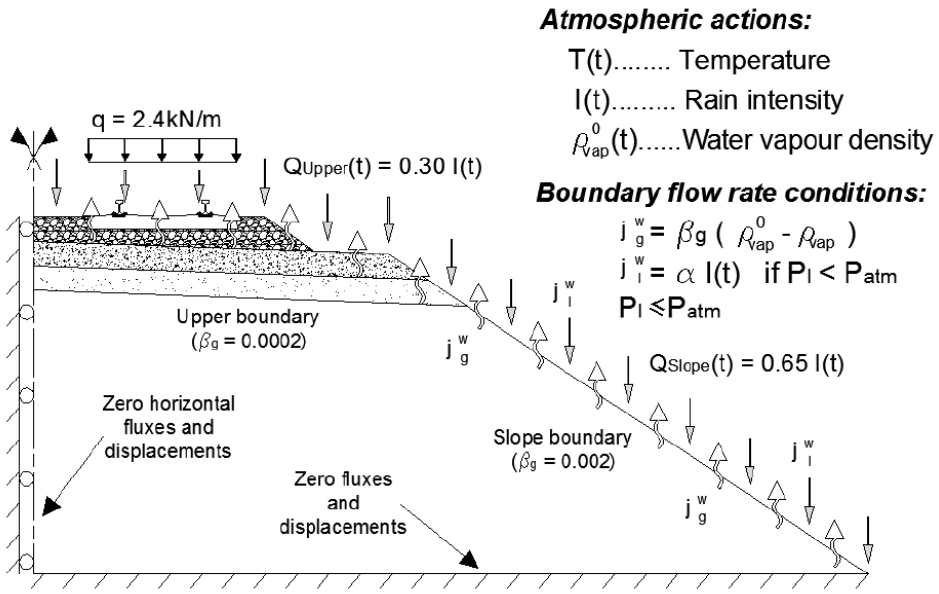

Figure 19 Boundary conditions

4.3.4 Construction Stages

The analysis has been classified into 5 construction stages namely;

- Stage 1: Initial Steady-State
- Stage 2: Insitu Condition
- Stage 3: Embankment Construction
- Stage 4: Service
- Stage 5: Service + Rainfall Event

4.3.5 Climate Data

Design return times in hydrology can range from 10 years to 100 years, and in nations (or locations) where the Probable Maximum Precipitation (PMP) has not been established, they can even reach 10,000 years. The choice of return period is influenced by several variables, including: (a) the drainage area's size; (b) the danger of failure; (c) the significance of the structure; and (d) the desired level of design conservatism.

Table 15 Guidelines for the selection of return period

No.	Type of project or feature	Return period (yr)
1	Urban drainage [low risk] (up to 100 ha)	5 to 10
2	Urban drainage [medium risk] (more than 100 ha)	25 to 50
3	Road drainage	25 to 50
4	Principal spillways (dams)	25 to 100
5	Highway drainage	50 to 100
6	Levees [medium risk]	50 to 100
7	Urban drainage [high risk] (more than 1,000 ha)	50 to 100
8	Flood plain development	100
9	Bridge design (piers)	100 to 500
10	Levees [high risk]	200 to 1000
11	Emergency spillways (dams)	100 to 10,000 (PMP)
12	Freeboard hydrograph [for a class (c) dam]	10,000 (PMP)

The lowest return period, applicable in urban drainage, is 5 to 10 years. Typically, these return periods are associated with drainage areas smaller than 100 ha (247 ac). When it comes to small watershed hydrology, the intensity-duration-frequency (IDF) curve that is appropriate is used to relate the peak discharge to both the duration and intensity of the rainfall. Small drainage areas concentrate quickly, leading to high intensities and, as a result, large peak discharges per unit of area. But because the area is so small, the peak discharge will also be so little. A high-intensity precipitation event is less likely to pass through a drainage area that is smaller. Therefore, it is typically not cost-effective to design for extended return durations for tiny areas with a time of concentration measured in minutes.

Table 16 IDF values generated.

Return Period (Years)	Duration (Minutes)	Intensity (mm/hr)
100	30	50.78
	60	32.17
	90	23.69
	120	18.82
	150	15.64
	180	13.40
50	30	29.56
	60	18.73
	90	13.79
	120	10.95
	150	9.10
	180	7.80
25	30	22.70
	60	14.38
	90	10.59
	120	8.41
	150	6.99
	180	5.99
10	30	17.36
	60	11.00
	90	8.10
	120	6.43
	150	5.35
	180	5.99
5	30	14.70
	60	9.31
	90	6.86
	120	5.45
	150	4.53
	180	3.88
2	30	12.72
	60	8.06
	90	5.94
	120	4.71
	150	3.92
	180	3.36

For highway/railway drainage design, the choice of return period depends on the importance of the structure. Return periods in highway and other regional transportation infrastructure, including culverts, typically vary from 25 to 100 yr. It is unusual for highway drainage to use return periods longer than 100 yr. The return period of 100 yr amounts to four human generations. It is a number which is not too high, nor too low. The value of 100 yr does not mean that the structure will be at risk exactly every 100 yr. Rather, it means that the structure will be at risk, say 10 times every 1000 years. As a rule, the larger the drainage area, the longer the return period. Typically, drainage areas less than 250 hectares do not warrant return periods greater than 25 years. However, larger areas, up to 10,000 hectares and beyond, may justify return periods up to 100 years or longer. (Fortunatoa, Oliveria, & Mazzola, 2014)

Ethiopia, broadly speaking has three seasons. The short rainy season, known as the Belg, runs from February to May. This is then followed by the long rainy season, known as the Kiremt, which is between June and September. The Bega, typically occurs between October and January, and is characterized by generally dry weather over the bulk of the country, with wet weather and a secondary peak in rainfall over the south.

4.4 Infiltration

The role of water infiltration in soil and the subsequent pore pressure response at depth are critical for understanding the transient conditions that lead to slope failure (Lu and Godt, 2013). Since soil is a mixture of solids with voids that are filled by fluids such as air and water, to exactly interpret the infiltration of rainfall through the slope surface, a fully coupled formulation of the water and air flow and the stress-strain behavior of soil should be considered.

When rainfall infiltration occurs through pore space in an unsaturated region, the flow of air also occurs, or the air is compressed by the interaction at the water-air interface. It is well known, based on experiments and analyses, that the flow of air through the pore space in unsaturated soil affects the infiltration of water (Touma and Vauclin, 1986; Sun et al., 2015). However, because of the difficulties of measuring pore-air pressure and analyzing air flow, the air flow induced by rainfall is ignored in general slope stability analyses by setting the pore air pressure to zero (Sun et al., 2015).

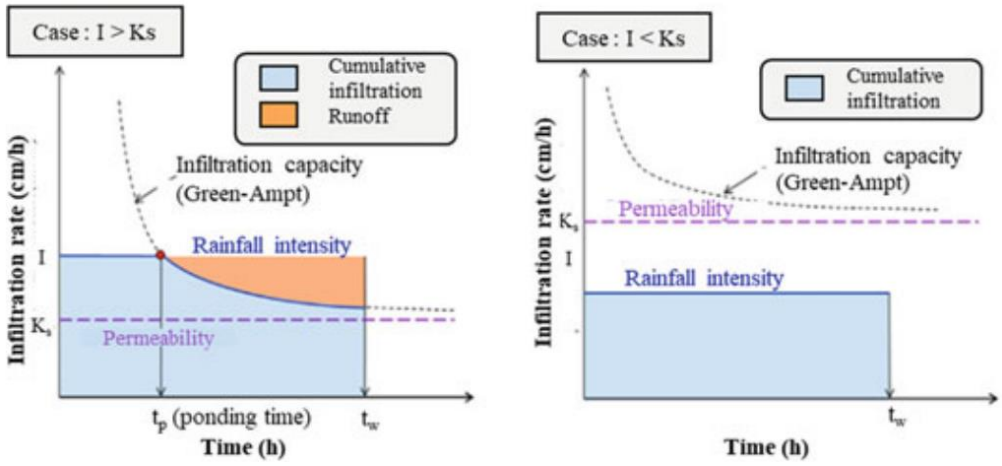

Figure 20 Infiltration rates (Mein and Larson (1973))

A Green and Ampt model (Green and Ampt 1911) that was modified by Mein and Larson (1973) has been used in this analysis. Groundwater flow analysis is performed on small unit volumes assumed to be homogeneous in soil characteristics. The fluxes are calculated to balance the masses of water entering to the unit volume and the water flowing out, satisfying Darcy's law.

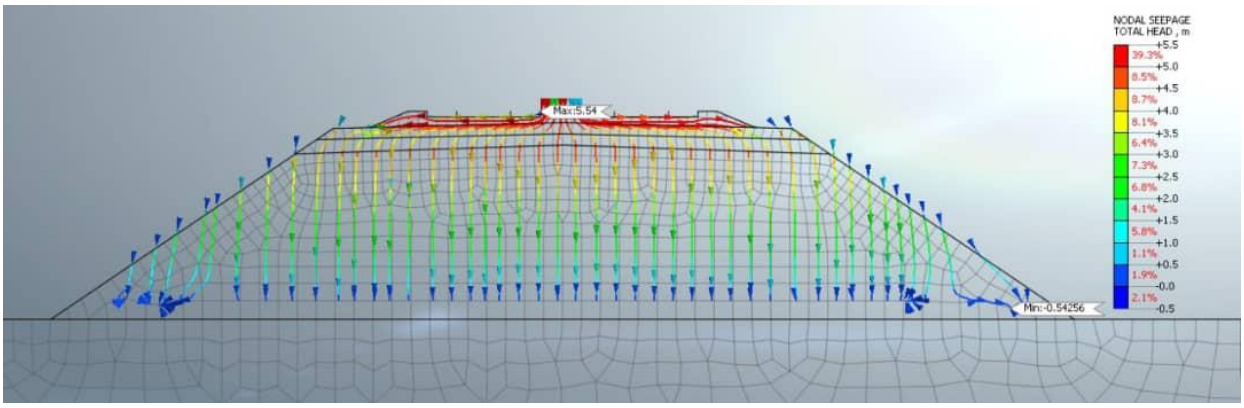

Figure 21 Infiltration modelling

The numerical model in the software utilized for the examination of the infiltration of rainfall into the embankment is shown in Figure 21. The basic instrument to determine the modification of mechanical characteristics of unsaturated soils with matric suction is the Soil-Water Characteristic Curve (SWCC), which was taken from a previous study. By placing a "unit flux, q" boundary on the top surface based on the associated rainfall from the updated IDF, rainfall was simulated. The infiltration capacity in the unsaturated zone is estimated using the formula of Green and Ampt (1911).

4.5 Matric Suction

Analysis was conducted to determine the seasonal variation of matric suction and the results from the analysis are presented in Table 10. It is observed that variation of matric suction during the drying cycle is different from the variation of matric suction during wetting cycle.

Table 17 Variation of matric suction simulation output

	Wetting Cycle						Drying Cycle					
Duration (minutes)	30	60	90	120	150	180	30	60	90	120	150	180
Precipitation (mm/hr)	50.78	32.17	23.69	18.82	15.64	13.40	26.45	16.76	12.34	9.80	8.15	6.98
Depth (m)												
0.0												
0.5												
1.0	75	85	90	93	95	100	87	99	130	155	180	205
1.5	72	82	88	91	94	99	84	95	128	154	179	204
2.0	69	81	86	89	92	97	83	90	126	152	177	202
2.5	67	79	85	87	91	95	81	89	124	151	175	200
3.0	65	77	83	86	89	94	79	87	123	149	174	199
3.5	63	76	80	85	87	93	78	84	122	147	173	198
4.0	61	73	78	82	85	89	75	82	119	145	169	194
4.5	60	71	76	80	83	85	73	80	117	143	165	190
5.0	59	70	74	78	81	83	72	78	115	141	163	188
5.5	58	68	73	76	79	82	70	77	113	139	162	187
6.0	56	67	72	75	78	80	69	76	112	138	160	185
6.5	55	66	71	75	77	79	68	75	112	137	159	184
7.0	53	65	70	74	76	78	67	74	111	136	158	183
7.5	50	64	69	73	75	77	66	73	110	135	157	182
8.0	49	61	68	72	74	76	63	72	109	134	156	181
8.5	48	59	65	71	73	75	61	69	108	133	155	180
9.0	47	58	63	68	72	74	60	67	105	132	154	179
9.5	46	57	62	66	69	73	59	66	103	129	149	174
10.0	45	56	61	65	67	70	58	65	102	127	143	165
10.5	43	55	60	64	66	68	57	64	101	124	138	153
11.0	39	54	59	63	65	67	56	63	100	115	127	142
11.5	38	50	58	62	64	66	52	62	96	104	116	131
12.0	37	49	54	61	63	65	51	58	88	93	105	120
12.5	36	45	53	57	62	64	47	57	84	86	94	109
13.0	35	43	49	56	58	63	45	55	73	79	83	98
13.5	34	39	47	52	57	59	41	52	69	75	79	84
14.0	33	36	43	50	53	58	34	47	57	59	68	72
14.5	30	34	38	41	52	54	26	33	44	49	54	60
15.0	25	30	35	40	45	50	25	30	35	40	45	50
15.5	23	27	32	36	41	45	23	27	32	36	41	45
16.0	20	24	28	32	36	40	20	24	28	32	36	40
16.5	18	21	25	28	32	35	18	21	25	28	32	35
17.0	15	18	21	24	27	30	15	18	21	24	27	30
17.5	13	15	18	20	23	25	13	15	18	20	23	25
18.0	10	12	14	16	18	20	10	12	14	16	18	20
18.5	8	9	11	12	14	15	8	9	11	12	14	15
19.0	5	6	7	8	9	10	5	6	7	8	9	10
19.5	3	3	4	4	5	5	3	3	4	4	5	5
20.0	0	0	0	0	0	0	0	0	0	0	0	0

It is also observed that the magnitude of matric suction during the drying cycle is higher than that of the wetting cycle. This confirms that the measurement and interpretation of SWCC of unsaturated soils needs to take into account the cycle (wetting or drying) of the specific problem being modelled.

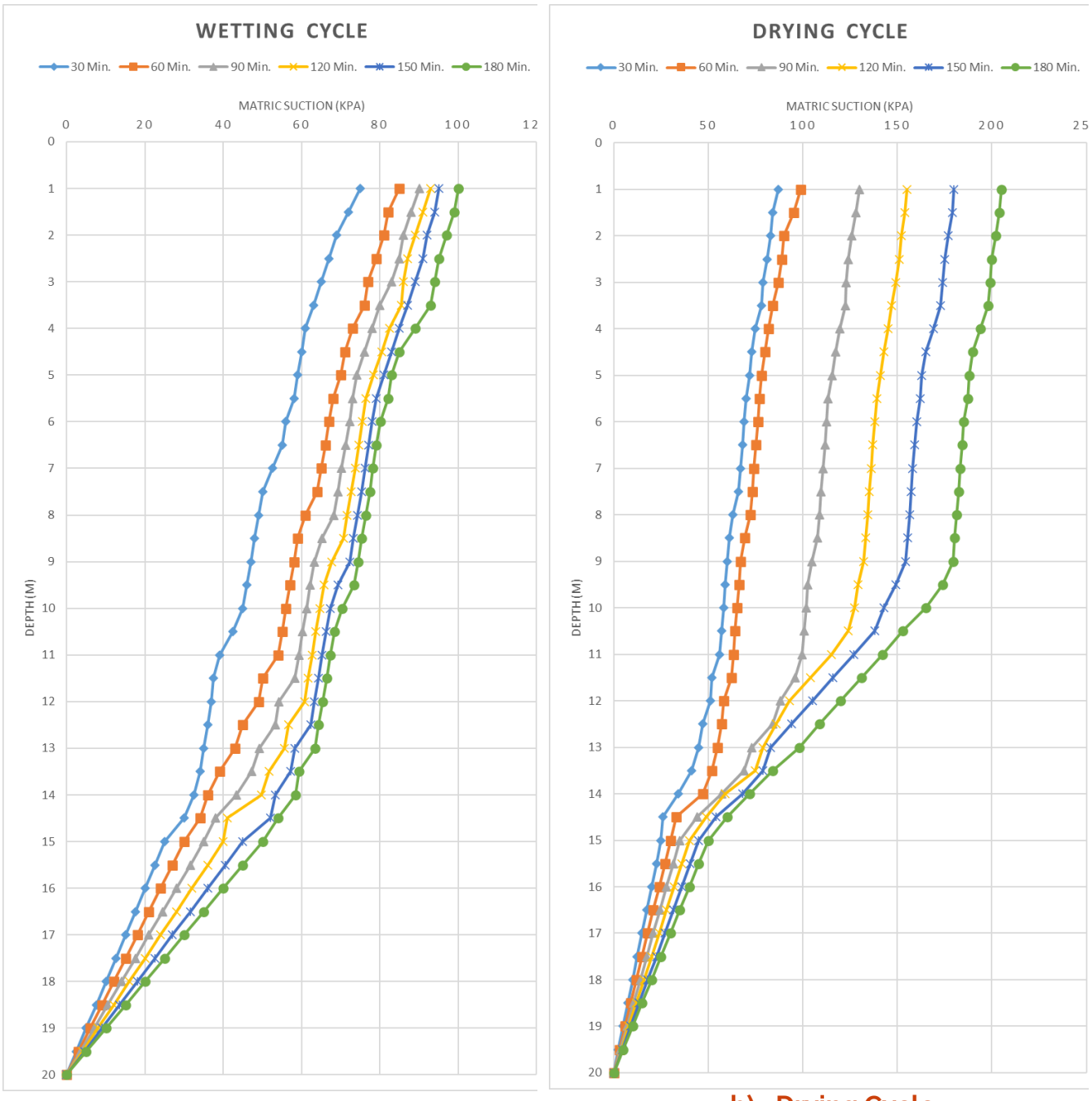

a) Wetting Cycle

b) Drying Cycle

Figure 22 Matric suction profile for 100YR return period.

Figure 22 present the variation of matric suction with depth corresponding to different rainfall duration for wetting and drying. It is observed that, in both cases, the magnitude of the matric suction diminishes with depth. It is also observed that the magnitude of the matric suction for rainfalls of higher duration is higher than that of rainfalls of lower duration, as for example, indicated by a matric suction value of 100 kPa (at a depth of 1 m below ground surface) for a duration of 180 min and 75 kPa (at a depth of 1 m below ground surface) for a rainfall duration of 30 min.

As can be noted from Figure 22, the evolution of the matric suction is consistent both spatially and temporally. It decreases with increasing depth and rainfall. The analysis's findings demonstrated that using data from environmental elements like rainfall observations, one can accurately estimate the change of matric suction in unsaturated soils. The pattern of matric suction variation with depth was effectively reflected by the predicted matric suction distribution profile. The findings suggest that over time, seepage analysis based on precise rainfall intensity data can deliver more accurate matric suction estimates.

4.6 Slope Stability

The results from the stability analysis are presented in Figure 20, Table 11 and Table 12. The factor of safety values are lower for rainfall of shorter duration. For example, the factor of safety for a rainfall duration of 30 min is 1.20 and that for 180 minutes is 1.89 for the wetting cycle. This indicates that the high intensity rainfall over a short duration has resulted in the highest decrease in matric suction and this led to loss of strength and hence to lower factor of safety. This is confirmed by the suction profile data presented in the previous section.

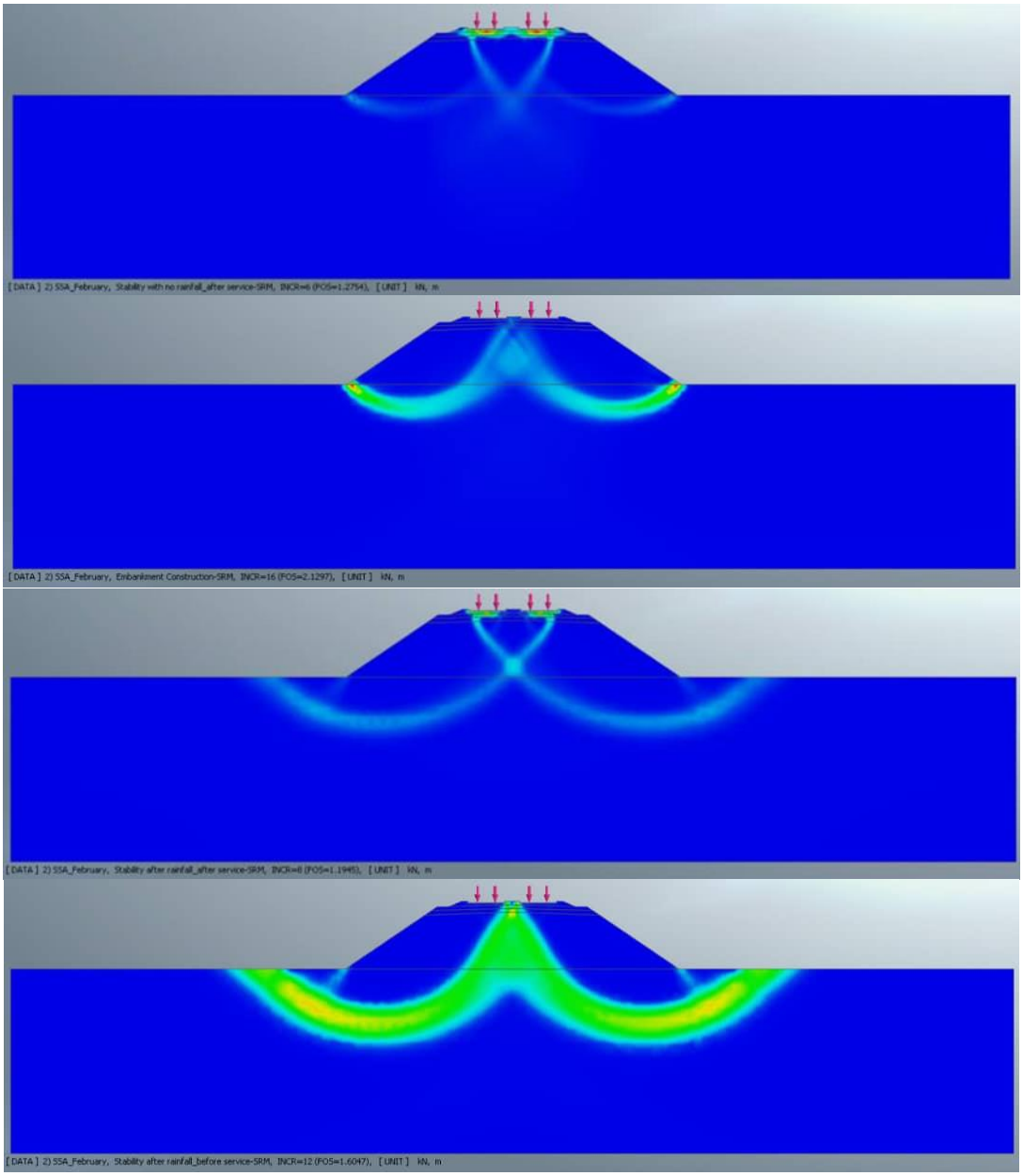

Figure 23 Evolution of slope stability for 100 YR return period.

Sample analysis output is presented in Figure 23. A summary of all slope stability analysis results is shown in Table 18.

Table 18 Factor of safety for 100 YR return period [6 rain durations]

	Wetting Cycle						Drying Cycle					
Duration (minutes)	30	60	90	120	150	180	30	60	90	120	150	180
Precipitation (mm/hr)	50.78	32.17	23.69	18.82	15.64	13.40	26.45	16.76	12.34	9.80	8.15	6.98
Factor of Safety	1.20	1.33	1.45	1.71	1.84	1.89	1.27	1.76	2.10	2.30	2.35	2.63

The effect of matric suction on slope stability of the embankment has two perspectives. If one chose to analyze using actual IDF values for each rain duration, factor safety improves with duration as depicted in Figure 24. It can also be noted that drying cycle enjoys a better factor of safety than the wetting cycle. Typically, during dry seasons, unsaturated soils have strong matric suction (i.e., negative pore-water pressure), which increases the soil's shear strength. The matric suction of the soil diminishes during lengthy rainy periods when there is adequate infiltration into the slope, which in turn causes an increase in the soil water content. As a result, the matric suction's added shear strength may be sufficiently diminished to cause a shallow landslide. (D. G. Fredlund, 2012)

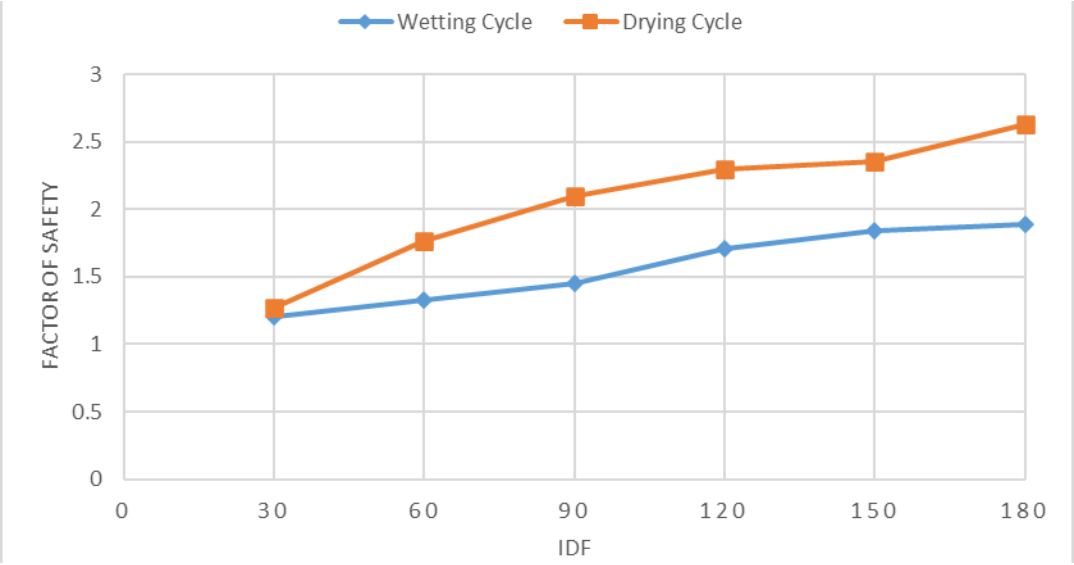

Figure 24 FS with actual IDF values

The result from actual IDF values may appear counterintuitive. A more sensible approach would be to find out how long will it take the slope to fail provided that the PMP is occurring; and the answer is 150 minutes i.e., 2.5 hours.

Table 19 Evolution of FS with PMP occurring over 6 rain durations.

Duration (minutes)	30	60	90	120	150	180
Precipitation (mm/hr)	50.78					
Factor of Safety	1.20	1.18	1.14	1.09	1.01	0.89

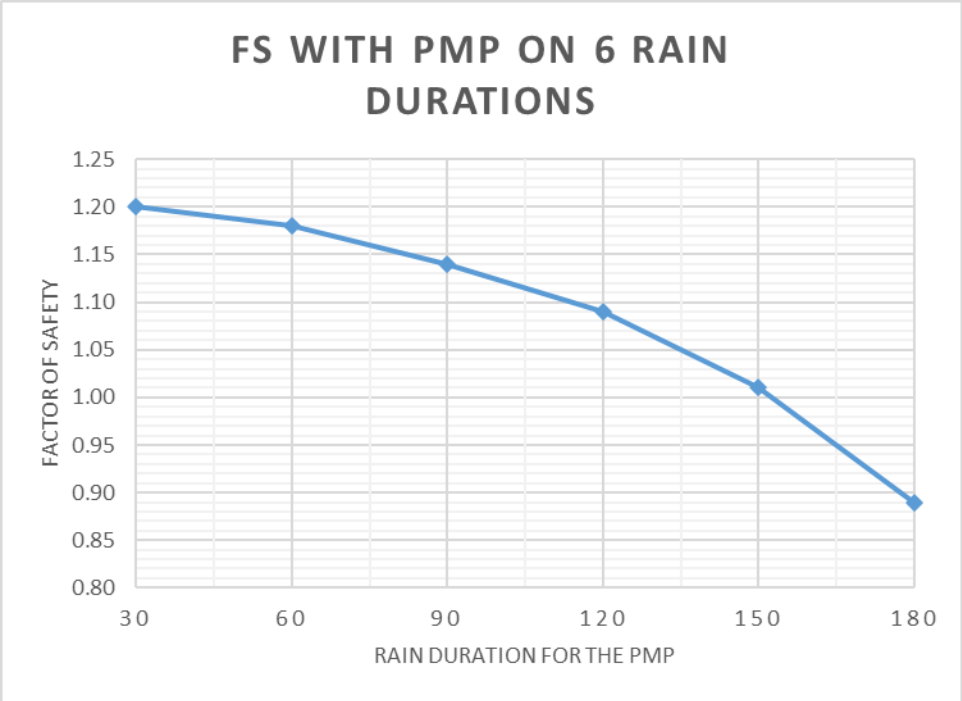

Figure 25 FS with PMP occurring over 6 rain durations.

Due to the drop in matric suction values brought on by the precipitation activity, the first local and general failures were noted late on the wetting cycle. During rain infiltration suction decreases and therefore the FOS of the slope is reduced.

4.7 Settlement

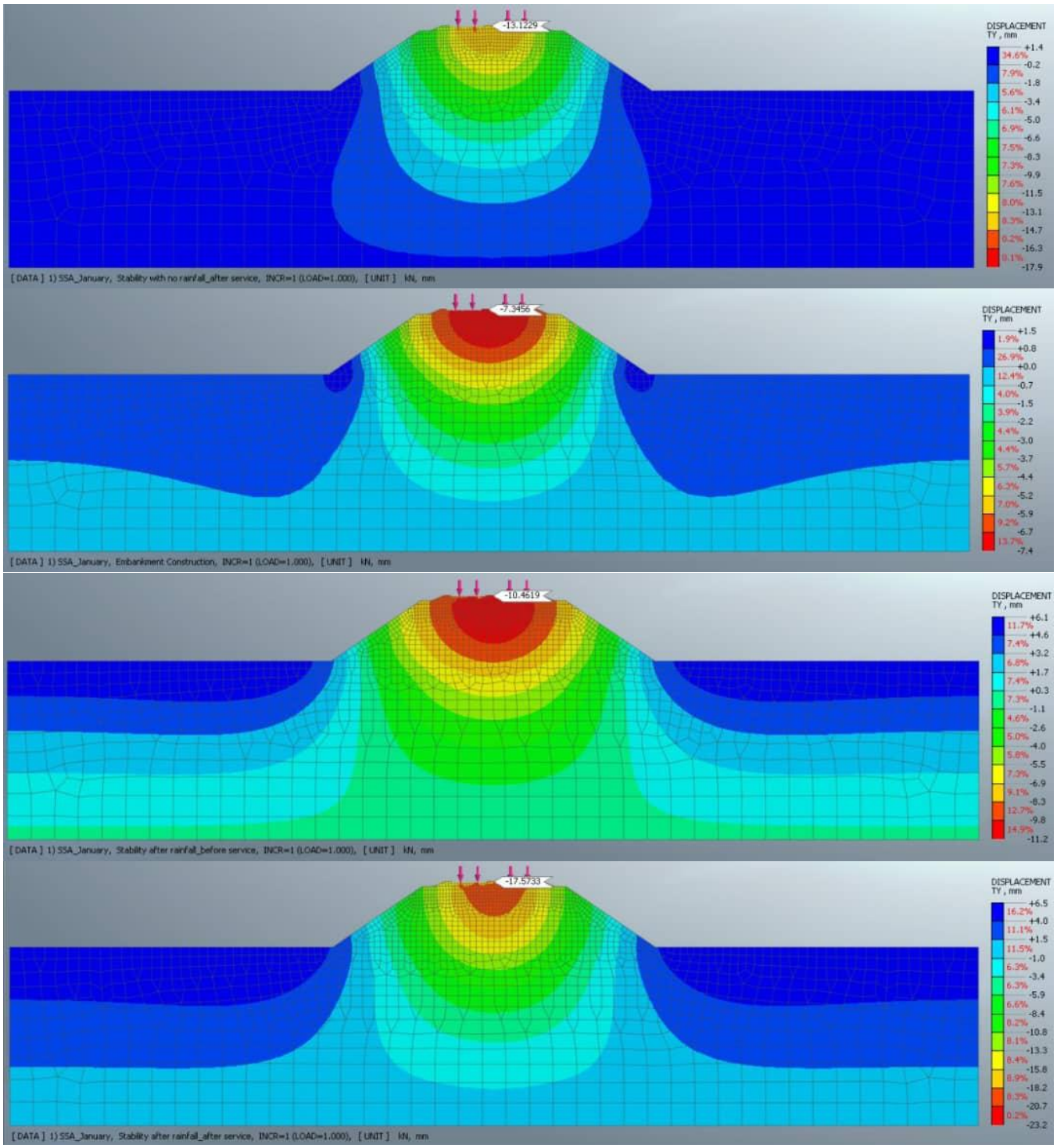

Figure 26 Evolution of settlement for 100 YR return period.

Sample analysis output is presented in Figure 26.

Table 20 Settlement values for 100 YR return period.

	Wetting Cycle						Drying Cycle					
Duration (minutes)	30	60	90	120	150	180	30	60	90	120	150	180
Precipitation (mm/hr)	50.78	32.17	23.69	18.82	15.64	13.40	26.45	16.76	12.34	9.80	8.15	6.98
Depth (m)												
0.0	90.7	67.2	49.4	41.5	35.6	33.7	56.8	44.9	36.5	27.2	26.8	21.4
2.5	66.6	61.6	45.0	39.3	34.3	32.1	50.2	40.2	32.4	25.4	24.5	20.8
5.0	58.5	51.9	36.6	33.0	29.0	26.4	39.5	35.5	25.2	19.6	18.2	16.1
7.5	43.1	36.6	32.8	28.7	25.3	23.3	36.6	32.1	24.2	19.0	17.9	15.1
10.0	34.8	33.3	25.0	20.3	17.6	16.1	29.6	24.7	19.2	14.3	13.5	10.1
12.5	25.6	22.2	19.6	18.4	17.5	15.5	19.6	18.3	16.2	13.4	12.6	10.7
15.0	18.4	17.1	16.2	14.4	13.3	10.8	15.6	13.9	9.2	8.4	7.7	7.3
17.5	6.2	5.6	5.1	4.2	3.6	3.4	8.8	7.3	5.6	4.7	3.9	2.7
20.0	0.0	0.0	0.0	0.0	0.0	0.0	0.0	0.0	0.0	0.0	0.0	0.0

As can be seen from Table 20, the maximum settlement (90 mm) occurs for the maximum precipitation amount (50 mm/hr).

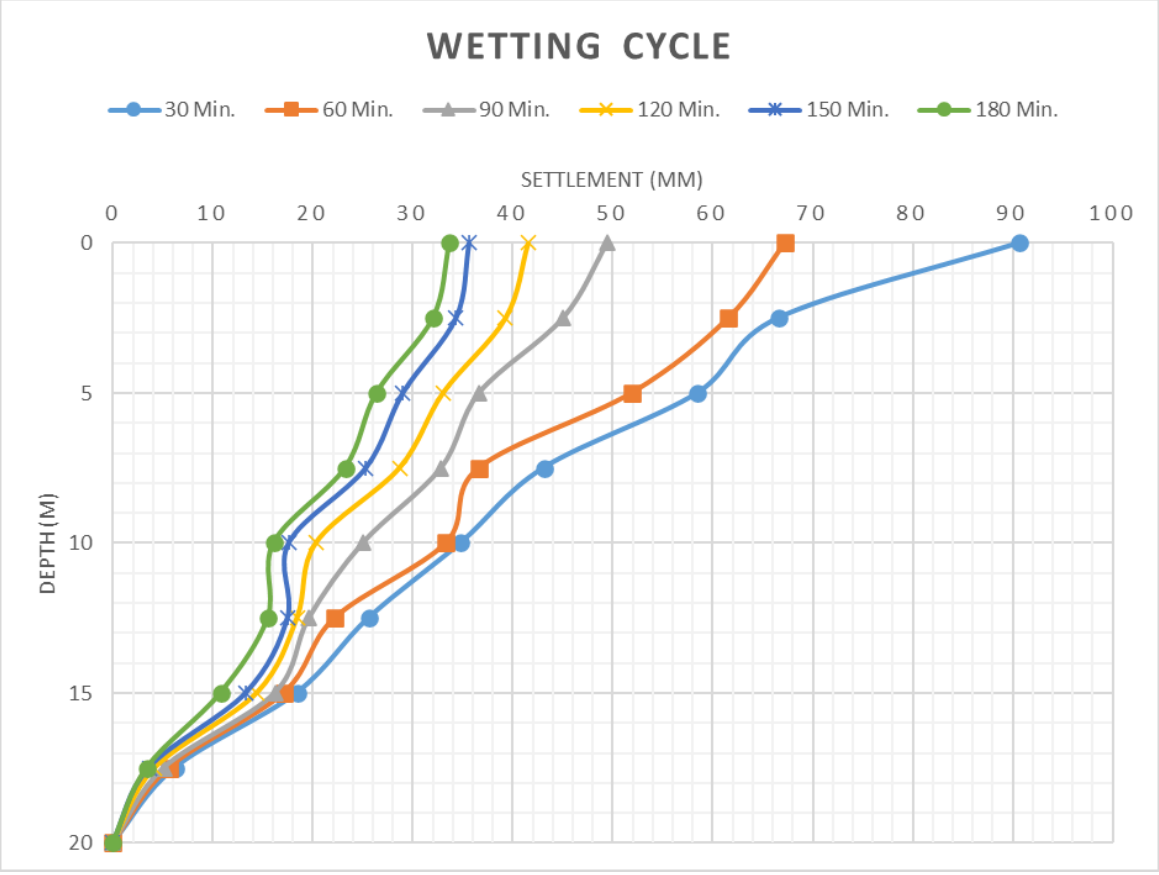

A) Wetting Cycle

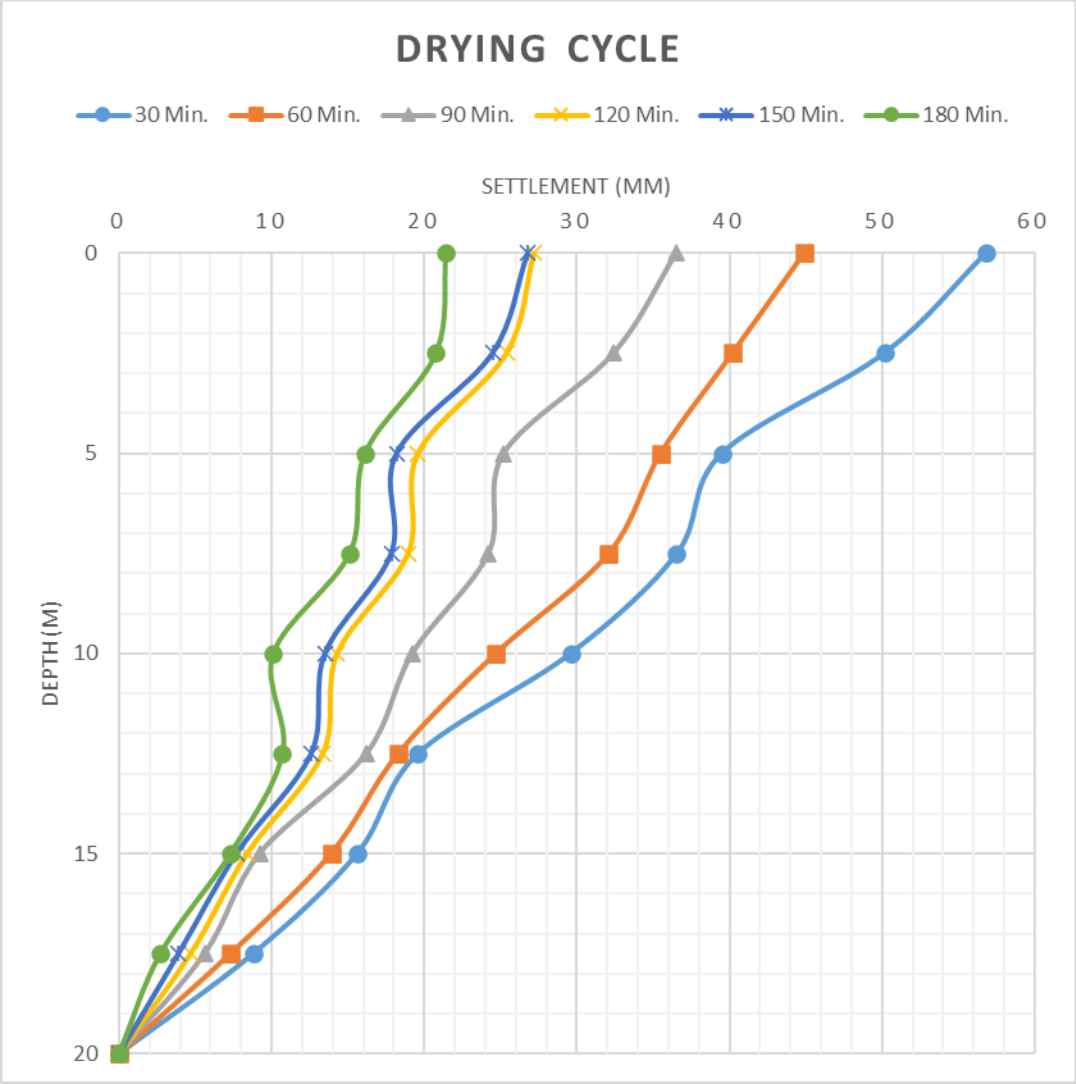

b) Drying Cycle

Figure 27 Settlement prediction as a result different IDF conditions

As per a variety of railway codes, the settlement should not exceed 50 mm under the allowable design load and not exceed 80 mm under 150% of the allowable design load. This means a 90 mm settlement is not acceptable and intervention is required to resume service of the railway line.

Settlement computation is a relatively tricky process since there are several actors in the play. Contributions from long-term settlements are not easy to quantify in such an analysis. The computed settlements due to rainfall induced influx give consistent results. They tend to decrease with an increase in depth and a decrease in rainfall duration.

4.8 Sensitivity of Results to Location of GWT

The location of the ground water table influences matric suction levels and variations. The location of the groundwater table in Addis Ababa is not clearly known. Several site investigations work in Addis Ababa report various levels ranging from 5 m to 15m. (Tensay GebreMedhin, 2023). This variation could be experienced by the railway track since it traverses from North to South of Addis Ababa passing through several locations of variable GWT. As such, sensitivity analysis was conducted by considering GWT of different depths 5 m. 10 m, and 15 m.

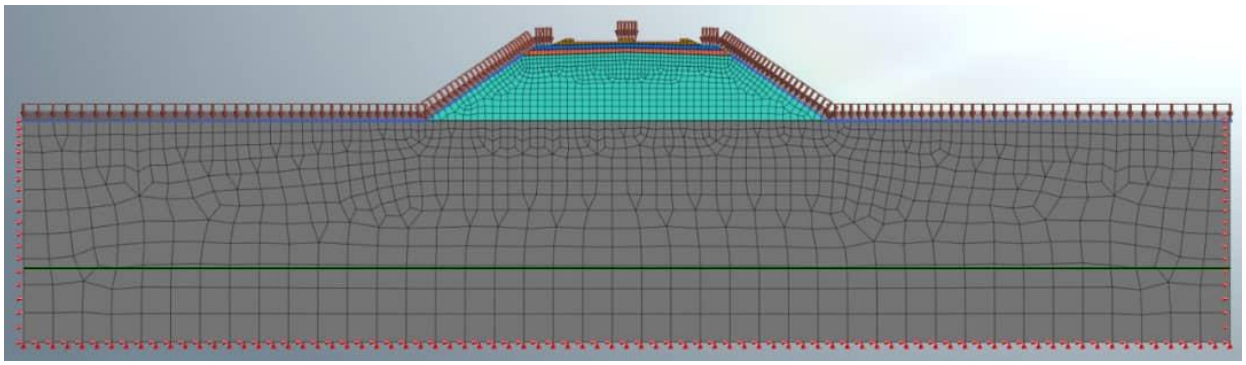

a) GWT located at 15 m.

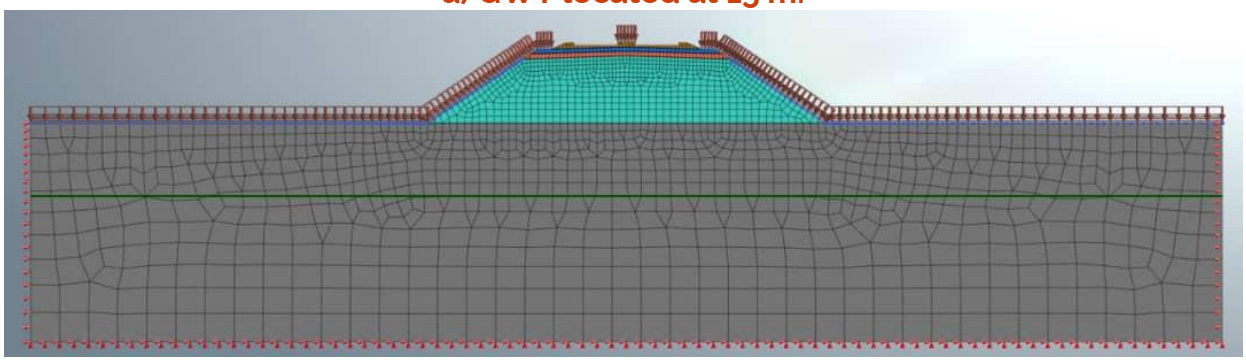

b) GWT located at 10 m.

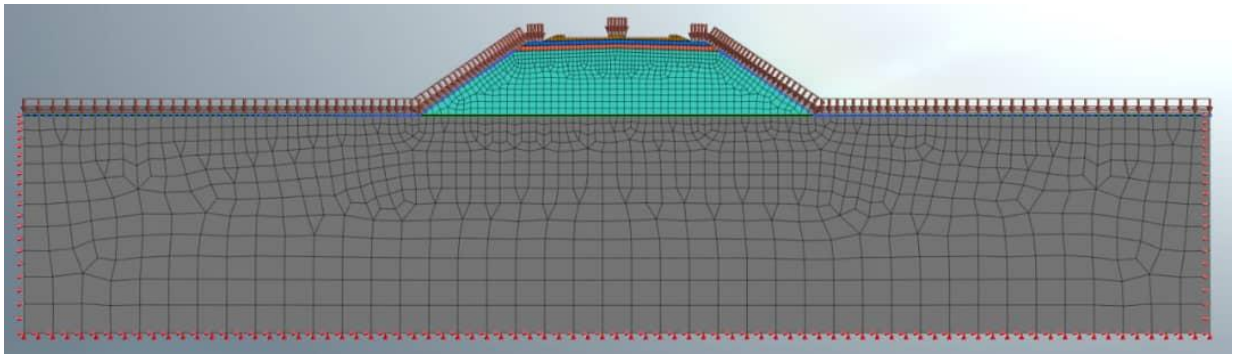

c) GWT located at 5 m.

Figure 28 Modelling of different GWT locations

	GWT		
Depth (m)	15 m	10 m	5 m
0.0			
0.5			
1.0	202.4	161.6	112
1.5	188.8	138.8	88.75
2.0	172.1	122.1	72.12
2.5	157.5	107.5	57.47
3.0	143.8	93.79	43.79
3.5	130.1	80.11	30.11
4.0	118.4	68.39	18.39
4.5	107.7	57.65	7.65
5.0	97.88	50	0
5.5	88.09	45	-5
6.0	80.26	40	-10
6.5	73.39	35	-15
7.0	67.47	30	-20
7.5	62.5	25	-25
8.0	58.47	20	-30
8.5	55.35	15	-35
9.0	53.14	10	-40
9.5	52.79	5	-45
10.0	50	0	-50
10.5	45	-5	-55
11.0	40	-10	-60
11.5	35	-15	-65
12.0	30	-20	-70
12.5	25	-25	-75
13.0	20	-30	-80
13.5	15	-35	-85
14.0	10	-40	-90
14.5	5	-45	-95
15.0	0	-50	-100
15.5	-5	-55	-105
16.0	-10	-60	-110
16.5	-15	-65	-115
17.0	-20	-70	-120
17.5	-25	-75	-125
18.0	-30	-80	-130
18.5	-35	-85	-135
19.0	-40	-90	-140
19.5	-45	-95	-145
20.0	-50	-100	-150

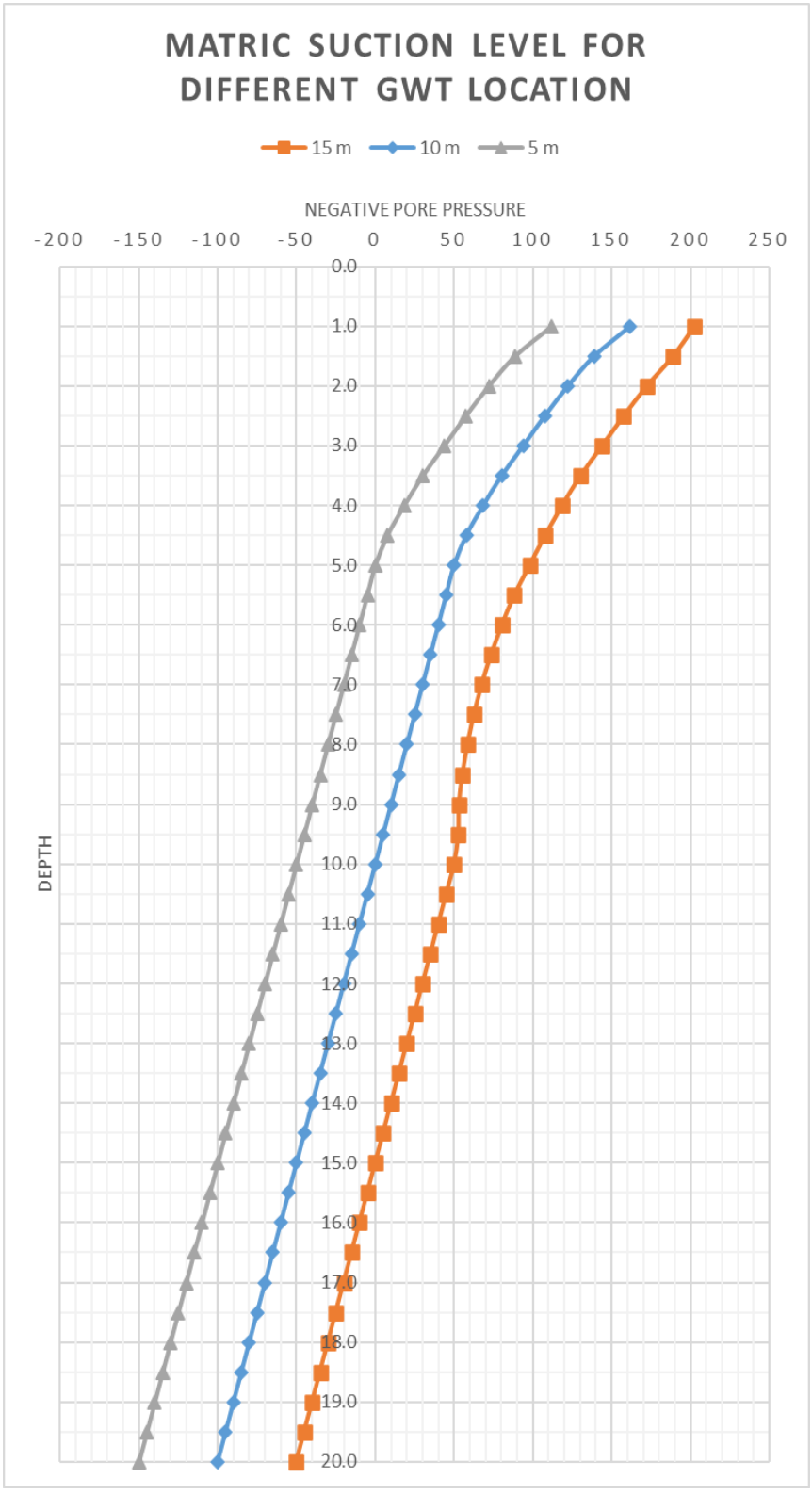

Figure 29 Matric suction level for different GWT locations

As can be seen from **Figure 29**, the matric suction level consistently decreases as GWT rises. This is very much in line with established literature. **(Hamdhan & Schweiger, 2011)**

Table 21 FS values for different GWT locations

GWT Location (m)	5	10	15	20
Precipitation (mm/hr)	50.78			
Factor of Safety	1.02	1.08	1.11	1.18

The minimum factor of safety is observed when the GWT is located at 5 m as stated in Table 21. This factor of safety is borderline failure value indicating that the location of GWT table has an influence that could potential extend to compromising overall stability of the embankment. The factor of safety decreases with decreasing depth of ground water table as depicted in Figure 30.

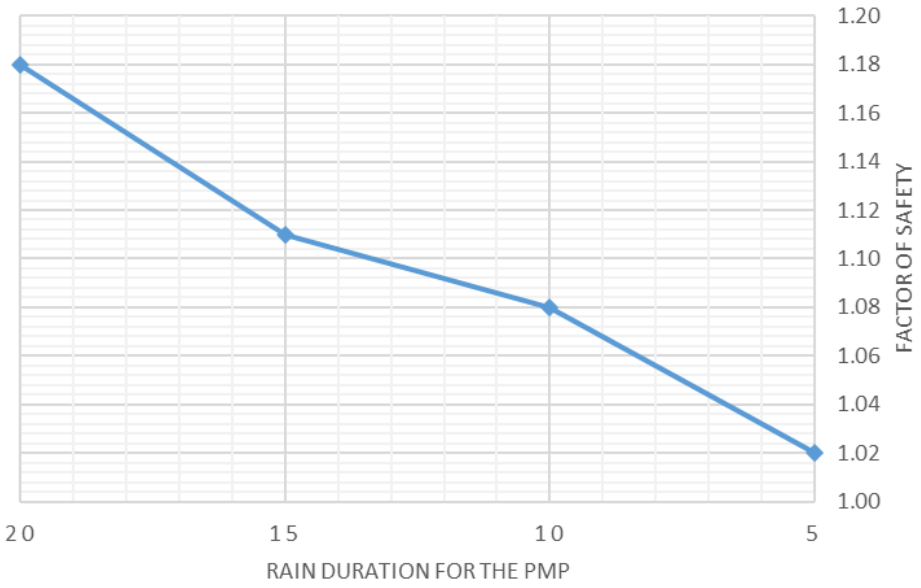

Figure 30 FS plot for different GWT locations

The settlement values corresponding to different GWT locations is presented in Table 22. Settlement consistently increases with rising ground water table as depicted in Figure 31. This result is very much in line with the established research literature. (Rafaela Cardoso, 2007)

Table 22 Settlement values for different GWT locations

GWT Location (m)	5	10	15	20
Precipitation (mm/hr)	50.78			
Depth (m)				
0.0	104.0	98.2	96.0	90.7
2.5	79.9	74.1	71.9	66.6
5.0	71.8	66.0	63.8	58.5
7.5	56.4	50.6	48.4	43.1
10.0	48.1	42.3	40.1	34.8
12.5	38.9	33.1	30.9	25.6
15.0	31.7	25.9	23.7	18.4
17.5	15.9	13.0	11.9	6.2
20.0	0.0	0.0	0.0	0.0

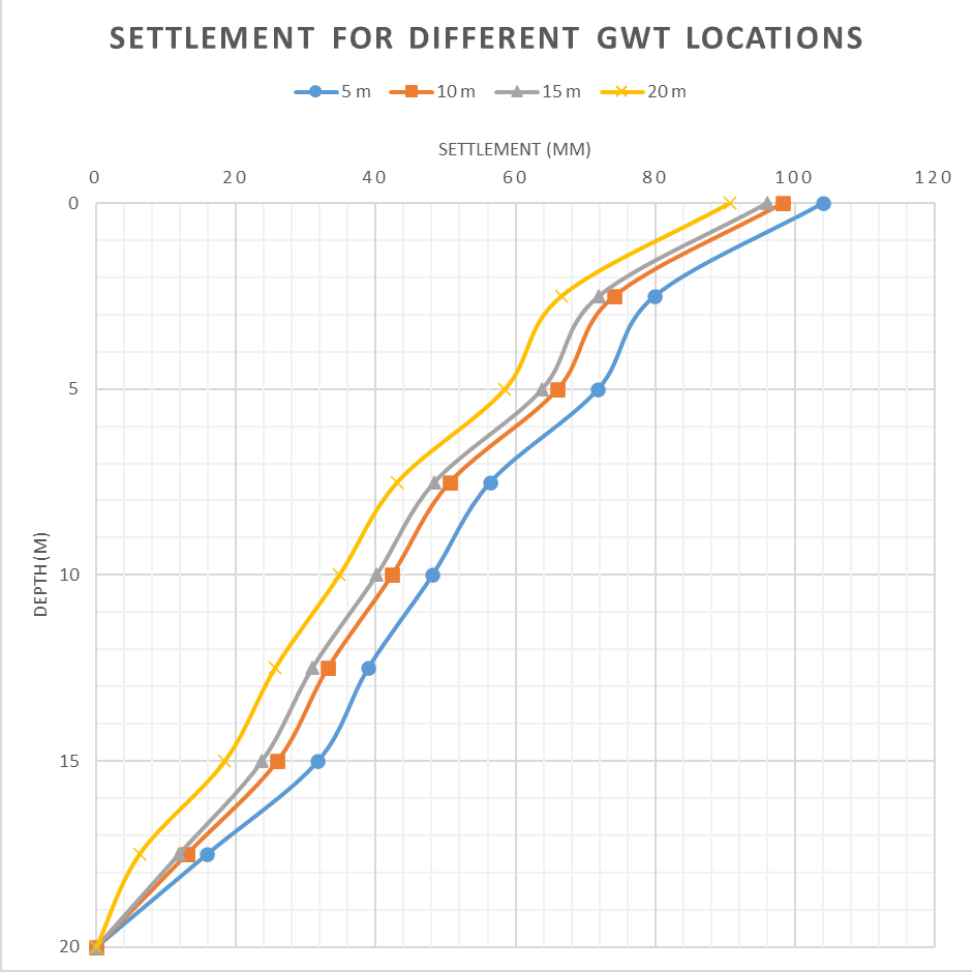

Figure 31 Settlement for different GWT locations

5. Conclusions and Recommendations

5.1 Conclusions

In this study, the researcher first set out to develop new and forward-looking rainfall and runoff IDF curves for Addis Ababa city using recently observed and projected precipitation and watershed data. Regional frequency analysis coupled with Bayesian uncertainty quantification and model averaging methods have been used to develop and update the rainfall IDF curves, which are then used in hydrologic model to develop the runoff IDF curves that explicitly account for effects of climate change into the IDF curves and related designs. This study aimed to develop IDF curves under the future climate scenarios for Addis Ababa, which have been compared with the IDF curves under the current climate. The results show that a maximum PMP of 50.58 mm/hr is predicted for Addis Ababa while the study by (Francesco De Paola, 2014) has produced 62.8 mm/hr for 100-year return period. The slight discrepancy may be accounted for by the fact that other researchers used historical data from 1964 – 2010 while the current study used 1980 – 2022 recent data. Moreover, the earlier researchers the climate (rainfall) simulations over the period 2010–2050, provided by CMCC (Centro Euro-Mediterraneo sui Cambiamenti Climatici) in order to estimate the contingent influence of climate change on the IDF curves, while the current researcher used an updated dataset of 2023 – 2063.

In the second part of this study, an extended Mohr-Coulomb soil model in the MIDAS GTX NS software has been utilized to analyze the effect of precipitation on slope stability and settlement of a railway embankment along the North-South direction of the AALRT. The software implementation of the model was initially verified using an already published research on slope stability analysis of unsaturated soil. The program is then used for the numerical simulation of the seepage, stability, and displacement modelling for an actual railway embankment geometry with an assumed homogenous soil slope during rainfall infiltration, and the following conclusions are obtained:

- With the increase in rainfall intensity and increase in rainfall duration, matric suction level decreases.

- The stability of an unsaturated slope will be affected by the distribution of negative pore water pressures (suction). The slope stability increases when the shear strength contributed by matric suction is considered. This affects the initial FOS of the slope before rainfall infiltration. During the time of rain infiltration, suction decreases and thus the FOS of the slope reduces.
- Settlements induced solely out of rainfall induced infiltration are not easy to isolate and compute. However, the trend shows that with an increase in rainfall, settlement tends to increase as well. A maximum settlement of 90 mm is predicted for 50.58 mm/hr precipitation.
- As per a variety of railway codes, the settlement should not exceed 50 mm under the allowable design load and not exceed 80 mm under 150% of the allowable design load. This means a 90 mm settlement is not acceptable and intervention is required to resume service of the railway line.
- Factor of safety of railway embankment decreases with increasing rainfall duration for the case of PMP. When rainfall amounts are equal, rainfall intensity has a greater effect on the slope's internal seepage, stability, and displacement than rainfall duration does. Therefore, consideration should be given to short-term severe rainfall while assessing the stability of a slope. This finding is very consistent with the existing literature such as (Cai, et al., 2020)

The investigation's findings demonstrated that utilizing rainfall observations in the finite element analysis, it is possible to accurately anticipate how the matric suction distribution profile changes over time in an embankment.

The analysis's findings also indicate that one of the most crucial variables influencing rainfall infiltration for unsaturated slopes is rainfall intensity. The behavior of saturated-unsaturated seepage and the stability of various soil slopes as a function of rainfall intensity is an intriguing geotechnical engineering study topic. The current analysis considers a variety of rainfall intensities linked to a variety of return durations.

It has also been made apparent that matric suction (and by extension slope stability and settlement) is highly affected by the location of ground water table. The factor of safety is amplified with raising depth of ground water table. Therefore, establishing the actual GWT is crucial in analysis and monitoring of actual embankments.

Rainfall is one of the most common triggers of slope failure because infiltration of rainwater into a slope increases the moisture content and weight of subsoil and reduces the suction and results in decrease in shear strength, thus making slopes unstable. Concepts from unsaturated soil mechanics were used in analyzing the impact of rainfall on the stability of railway tracks. This study has investigated the impact of rainfall on the stability of railway embankments. The results indicated that the slope stability and settlement of the railway embankments is affected by the rate and duration of rainfall. It has highlighted that the stability of the embankments is affected by rainfall indicating the need to consider climatic conditions, which could change drastically due to global warming, in the design and monitoring of the performance of railway tracks.

The effect of wetting and drying cycles on the suction profile, on the stability of the embankment slope, and on settlement of the embankments was also investigated. The results indicated that the wetting and drying cycles impact the performance of the railway embankment.

This study, in general, highlights the need to consider the performance of railway tracks and embankments by using concepts from unsaturated soil mechanics since the problem, in reality, is an unsaturated soil mechanics problem. It also highlighted the importance of climatic condition in assessing the performance of railway tracks.

5.2 Recommendations

Future researchers can build up on the current research by adding the following components.

- Employ field monitoring technics to verify settlement predictions,
- Use of physical model and testing to verify stability analysis outputs for worst case scenarios,
- Taking actual soil sample from the embankment,
- Consider calibration and utilization of an elasto-plastic unsaturated soil model (such as the BBM) for further study,

The water retention curve of a soil evolves during compaction because the volume of pores decreases, pore sizes change, and the proportion of the void space in micro and macro pores changes. Another researcher may consider including this dimension in further study. The effect of matric suction accumulation can also be another area of improvement for further studies.

Without completing field research at several locations with various slopes and being aware of the subsoil's strength characteristics, this is not very simple. A comprehensive study is recommended for the AA LRT and other railway network of the country to bridge the gap in available data and devise a comprehensive monitoring scheme, Surface cracks, which are brought on by slight slope displacement, are known to precede slope failure. As such, empiricism and human observation also play a critical role in avoiding calamity.

Many public sectors elsewhere have embraced the rainfall-based strategy, and a regional early warning has been released. The absence of geological, topographical, and geotechnical consideration are the potential limitations for the adoption of the rainfall criterion in Ethiopia. As a result, it is impossible to determine whether a specific slope will be unstable during a strong downpour. Monitoring soil moisture levels can detect the beginnings of a slope failure since higher soil moisture levels weaken the soil's ability to

resist shear. However, it is necessary to monitor the slip surface's moisture content for this reason.

Transportation route is a typical linear infrastructure in which damage at one point affects the operation of the entire route. As such, due attention should be given to such mega investments through deployment of monitoring schemes and research collaboration with academic institutions. The Ethiopian Railway Corporation should consider monitoring its embankments, accumulate data, draw out trends and employ a rainfall-based criterion for decision making whether or train service is stopped and to resume train operation after heavy rain.

References

A. S. O'Brien, E. A. (2004). Old Railway Embankment Clay Fill - Laboratory Experiments, Numerical Modelling and Field Behaviour. *Advances in Geotechnical Engineering: The Skempton Conference.* London: Thomas Telford.

Akalu, M. (2017). *Engineering Characteristics of Red Soil: A Case from Western Addis Ababa, Ethiopia.* College of Natural Sciences, School of Earth Science. Addis Ababa: School of Graduate Studies, Addis Ababa University. Retrieved from http://etd.aau.edu.et/bitstream/123456789/16300/1/Medhanit%20Akalu.pdf

Alonso, E. E. (1990). A constitutive model for partially saturated soils. *Géotechnique, 40(3)*, 405-430.

American Railway Engineering and Maintenance-of-Way Association. (2019). *Manual for Railway Engineering.* AREMA.

Anderson, M., & Pope, R. (1984). The incorporation of soil water physics models into geotechnical studies of landslide behaviour. *MG Anderson, RG Pope - Proceedings of the 4th International Symposium on Landslides Vol.4*, (pp. 349 - 355).

Antonio Gens, M. S. (2016). On constitutive modelling of unsaturated soils. *Acta Geotechnica*, 137-147. doi:DOI 10.1007/s11440-006-0013-9

Armen Ter-Martirosyan, V. S. (2019). Determining the interfaces parameters for geotechnical modelling. *Open Access proceedings in Environment, Energy and Earth Sciences.*

Blight, G. (1997). Interactions between the atmosphere and the Earth. *Geotechnique*.

Buddhima Indraratna, Q. S. (2017). Behaviour of Subballast Reinforced with Used Tyre and Potential Application in Rail Tracks. *Transportation Geotechnics*.

Cai, G., Li, M., Han, B., Di, K., Liu, Q., & Li, J. (2020). Numerical Analysis of Unsaturated Soil Slopes under Rainfall Infiltration Based on the Modified Glasgow Coupled Model. *Advances in Civil Engineering*.

Chemonics International Inc. (2015). *Climate Change Variability and Change in Ethiopia: Summary of Findings.* Washington DC: United States Agency for International Development. Retrieved from https://www.climatelinks.org/resources/climate-variability-and-change-ethiopia

Cho, S., & Lee, S. (2001). Instability of unsaturated soil slopes due to infiltration. *Computers and Geotechnics 28*, 185 - 208.

D. G. Fredlund, H. R. (2012). *Unsaturated Soil Mechanics in Engineering Practice.* Hoboken, USA, New Jersey: John Wiley & Sons Inc.

Daichao Sheng, A. G. (2008). Unsaturated soils: From constitutive modelling to numerical algorithms. *Computers and Geotechnics, 35*, 810-824.

Fortunatoa, A., Oliveria, E., & Mazzola, M. R. (2014). Selection of the Optimal Design Rainfall Return Period of Urban Drainage Systems. *16th Conference on Water Distribution System Analysis, WDSA 2014* (pp. 742-749). Procedia Engineering.

Francesco De Paola, M. G. (2014). Intensity-Duration-Frequency (IDF) rainfall curves, for data series and climate projection in African cities. *SpringerPlus*.

Hamdhan, I. N., & Schweiger, H. F. (2011). Slope Stability Analysis of Unsaturated Soil with Fully Coupled Flow-Deformation Analysis. *Mathematical Geosciences at the Crosroads of Theory and Practice.* Salzburg, Austria: International Association for Mathematical Geosciences (IAMG).

Ismail, N. (2013). *Prediction of Soil Water Characteristic Curves based on Grain Size Distribution and Plasticity Index for Red Clay and Expansive Soils found in Addis Ababa.* Addis Ababa Institute of Technology, Department of Civil Engineering. Addis Ababa: School of Graduate Studies of Addis Ababa University. Retrieved from http://etd.aau.edu.et/bitstream/123456789/4310/2/NURU%20ISMAIL.pdf

J.M. Scott, F. L. (n.d.). *Influence of climate and vegetation on railway embankments.* United Kingdom: Mott MacDonald.

Jean-Louis Briaud. (2013). *Geotechnical Engineering: Unsaturated and Saturated Soils.* Hoboken, USA, New Jersy: John Wiley & Sons.

Lam, L., Fredlund, D. G., & Barbour, S. L. (1987). Transient seepage model for saturated–unsaturated soil systems: a geotechnical engineering approach. *Canadian Geotechnical Journal Vo. 24 No. 4*.

Likos, N. L. (2004). *Unsaturated Soil Mechanics.* Hoboken, USA, New Jersey: John Wiley & Sons.

Lloret-Cabot, M., Wheeler, S. J., & Sánchez, M. (2017). A unified mechanical and retention model for saturated and unsaturated soil behaviour. *Acta Geotechnica*, 1 - 21.

Lyon Associates Inc. & Building and Road Research Institute. (1971). *Laterite and Lateritic Soils and Other Problematic Soils of Africa.* Kumasi, Ghana: Agency for International Development.

Muluneh, Y. (2012). *Correlation between Critical State Soil Parameters and Index Properties of Remolded Red Clay Soils of Addis Ababa.* Addis Ababa Institute of Technology, Department of Civil Engineering. Addis Ababa: School of Graduate Studies of Addis Ababa University.

Ng, C. W., & Shi, Q. (1998). A Numerical Investigation of the Stability of Unsaturated Soil Slopes Subjected to Transient Seepage. *Computers and Geotechnics, Vol. 22, No. 1*, 1 - 28.

Ni An, S. H. (2017). Numerical analysis of soil volumetric water content and temperature variations in an embankment due to soil-atmosphere interaction. *Computers and Geotechnics 83 (2017)*, 40-51.

Oh, W. T., Vanapalli, S. K., Qi, S., & Han, Z. (2016). Estimation of the variation of matric suction with respect to depth in a vertical unsaturated soil trench associated with rainfall infiltration. *3rd European Conference on Unsaturated Soils.*

Pradel, D., & Raad, G. (1993). Effect of Permeability on Surficial Stability of Homogeneous Slopes. *Journal of Geotechnical Engineering Vol. 119 Issue 2*.

R Cardaso, V. F. (2015). Influence of atmospheric action on the performance of railway embankments built with different subgrade soils. Kyoto: CRC Press.

Rafaela Cardoso, V. F. (2007). Settlement Prediction of High Speed Railway Embankments Considering the Accumulation of Wetting and Drying Cycles. *Experimental Unsaturated Soil Mechanics*, 291 -298.

Rahardjo, D. G. (1993). *Soil Mechanics for Unsaturated Soils.* Hoboken, USA, New Jersey: John Wiley & Sons Inc.

Riad, B., & Zhang, X. (2020a). Modified State Surface Approach to Study Unsaturated Soil Hysteresis Behavior. *Transportation Research Record: Journal of the Transportation Research Board*, 484 - 498.

Riad, B., & Zhang, X. (2020b). Using Modified State Surface Approach to Study the Hydro-Mechanical Behavior of Unsaturated Soils. *Geo-Congress*, 377 - 386.

S. Glendinning, J. W. (2009). Asset-management strategies for infrastructure embankments. *Proceedings of the Institution of Civil Engineers - Engineering Sustainability Volume 162 Issue 2*, (pp. 111-120). London.

S. Glendinning, P. H. (2014). Construction, management and maintenance of embankments used for road and rail infrastructure: implications of weather induced pore water pressures. *Acta Geotechnica*.

S. K. Vanapalli, W. O. (2012). Stability Analysis of Unsupported Vertical Trenches in Unsaturated Soils. *GeoCongress* (pp. 2502-2511). Oakland, California: Geo-Institute of American Society of Civil Engineers.

Schanz, T. (2007). *Theoritical and Numerical Unsaturated Soil Mechanics.* Springer-Verlag Publishing.

Scott Socolofsky, E. A. (2001). Disaggregation of Daily Rainfall for Continuous Watershed Modeling. *Journal of Hydrologic Engineering Vol. 6, No. 4*, 300 - 309.

Sheng, D. (2011). Constitutive modelling of unsaturated soils: Discussion of fundamental principles. *Unsaturated Soils*, 91 - 112.

Sheng, D., Fredlund, D. G., & Gens, A. (2008). A new modelling approach for unsaturated soils using independent stress variables. *Canadian Geotechnical Journal*.

Sivakumar, E. J. (2010). *Unsaturated Soils: A fundamental interpretation of soil behaviour.* Chichester, United Kingdom, West Sussex: Wiley_Blackwell.

Tensay GebreMedhin, T. G. (2023). *Assessment of Contemporary Geotechnical Engineering Practice in Ethiopia with a Focus on Site Investigation Works in Addis Ababa.* Addis Ababa: Unpublished.

Thomas, H. R., & Rees, S. W. (1994). Seasonal ground movement in unsaturated clay: an examination of field behaviour. *Géotechnique Volume 44 Issue 2*, 353-358.

Tirualem, A. (2012). *Effect of strain rate on stress-strain relationship and shear strength of Addis Ababa red clay.*

Vahedifard, F., & Robinson, J. D. (2015). Unified Method for Estimating the Ultimate Bearing Capacity of Shallow Foundations in Variably Saturated Soils under Steady Flow. *Journal of Geotechnical and Geoenvironmental Engineering*.

Valerie Whenham, M. D.-C. (2007). Influence of Soil Suction on Trench Stability. In T. Schanz (Ed.), *International Conferences on Unsaturated. Springer Proceedings in Physics*, pp. 495-501. Weimar: Springer.

W/Medhin, G. (2010). *A Study on Shear Strength Characteristics of Addis Ababa Red Clay Soil for Unsaturated Case.* Faculity of Technology, Department of Civil Engineering. Addis Ababa: School of Graduate Studies of Addis Ababa University.

Wood, D. M. (1990). *Soil Behaviour and Critical State Mechanics.* Cambridge University Press.

Woto, S. S., & Azmatch, T. F. (2022). *Soil-Water Characteristic Curve for Red Clay Soils of Addis Ababa.* Addis Ababa, Ethiopia: Thesis Work at Addis Ababa Institute of Technology.

Y.J. Cui, Y. G. (2010). Simulating the water content and temperature changes in an experimental embankment using meteorological data. *Engineering Geology*, 456-471.

Zhang, X., & Lytton, R. L. (2009a). Modified state-surface approach to the study of unsaturated soil behavior. Part I: Basic concept. *Canadian Geotechnical Journal*, 536 - 552.

Zhang, X., & Lytton, R. L. (2009b). Modified state-surface approach to the study of unsaturated soil behavior. Part II: General formulation. *Canadian Geotechnical Journal*, 553 - 570.

Zhigang Cao, Q. Z. (2020). The effects of suction history on the cyclic behavior of unsaturated road base filling materials. *Elseveir - Engineering Geology*.